

# **Fabrication and Characterization of Laser Scribed Flexible Supercapacitor**



Name: Tayyaba Malik

Reg. No: 119604

**This thesis is submitted as a partial fulfillment of the requirements for  
the degree of**

**MS in Nanoscience and Engineering**

**Supervisor Name: Dr. Mohammad Ali Mohammad**

**School of Chemical and Materials Engineering (SCME)  
National University of Sciences and Technology (NUST)**

**H-12 Islamabad, Pakistan**

**November, 2018**

# **Dedication**

**Dedicated**

*To all those without whom this research journey would not have been possible;*

*My Family*

*&*

*Those Teachers, Mentors & Friends*

*Whose firm belief in me,*

*Has been the driving force in my life!*

*Their unconditional love, support and prayers remain my remitting source of strength*

## Acknowledgements

All praise to Almighty **ALLAH**, the most Gracious and Benevolent and His last Prophet Muhammad (Peace be upon him) whom Allah exalted as the best source of guidance and knowledge for humanity.

I would like to thank my supervisor Dr. Mohammad Ali Mohammad for his guidance, dedication, keen interest and for doing every possible help. I have been very lucky to have a supervisor who responded to my questions and queries on time. Without his personal supervision, advice and valuable guidance, completion of my project would have been doubtful. I am thankful to him for keeping me highly motivated throughout my degree journey and making me understand how hard work and determination never go unrewarded.

I would also like to pay my deepest gratitude to my GEC members Dr. Zakir Hussain and Dr. Iftikhar Hussain Gul for helping me. I achieved my tasks under the light of their knowledge. I also express my gratitude to Dr. Aslam Baig (NCP) and Dr. Usman Liaqat for all their guidance during the course of this project especially in characterization of laser. I further would like to extend my thanks to Dr. Rizwan Hussain, Dr Aftab Akram and Engr. Mudassar Shazad for their helpful advices and insight. I would also like to show my gratitude towards Principal SCME and HoD Materials Engineering Department for administrative support. I would also like to thank Lab staff of SCME who helped me in all possible manners.

I am thankful to my friends Aqsa Aziz, Ayesha Pervaiz and Tayyaba Nosheen for always listening, supporting and encouraging me. I am also thankful to my research fellows Shayan Naveed, Hinna Jamil, Farheen Nasir and Sadaf Batool who helped me during lab.

Finally, I would like to acknowledge and thank my Mother, my Sisters, my Brother and my Husband without their prayers, encouragement and support it would not have been possible for me to complete my work. I am forever thankful for their prayers and love.

Tayyaba Malik

## Abstract

Recently, supercapacitors have attracted a tremendous amount of attention as energy-storage devices due to their high-power density, fast charge–discharge ability, excellent reversibility, and long cycling life. In this research work, we demonstrate a laser scribed super capacitor based on polyimide (PI) substrate for the storage of electrical energy. PI substrate of thickness 200 $\mu\text{m}$  and area 1 cm  $\times$  1 cm was reduced by a laser engraver with a 450 nm wavelength in the form of stackable supercapacitor electrodes. Although, PI itself exhibits non-conductive behavior; however, by laser irradiation we change the surface properties of PI and reduce its resistance. The chemical property of irradiated PI was characterized by using Raman, FTIR and XRD where the carbon peak was observed at  $2\theta = 25.44$  in case of XRD results, which confirms the reduction of PI material in to a graphene-like substance. The electrical conductivity was analyzed with a probe station and observed to be 1.6mS. Two conductive regions were assembled into a capacitor device by sandwiching different electrolytes (KOH/H<sub>2</sub>O, H<sub>3</sub>PO<sub>4</sub>/H<sub>2</sub>O, KOH+KI/PVA, H<sub>3</sub>PO<sub>4</sub>/PVA) in between. The best capacitance value was achieved by using the H<sub>3</sub>PO<sub>4</sub>/PVA as an electrolyte in between the electrodes. During the charging and discharging characterization of the capacitor device, current density was observed to be 1.5mA/cm<sup>2</sup>. When this supercapacitor capacitance versus voltage analysis was carried out and the device showed 75mF/cm<sup>2</sup> against a voltage sweep of  $\pm 2\text{V}$ . The galvanostatic charging and discharging curve shows a symmetric behavior with respect to time exhibiting the stability and durability of the device. At lower scan rate the capacitance value is higher but the value of current is lower. In this paper the device capacitance value is checked by changing the electrolyte, by changing the Scan rate and by changing the laser intensity. All these parameters effect the performance of the device.

# Table of Contents

<b>Dedication .....</b>	<b>i</b>
<b>Acknowledgements.....</b>	<b>ii</b>
<b>Abstract .....</b>	<b>iii</b>
<b>List of Figure.....</b>	<b>vii</b>
<b>List of Tables.....</b>	<b>x</b>
<b>Abbreviations.....</b>	<b>xi</b>
<b>Chapter 1: Introduction .....</b>	<b>1</b>
1.1 Flexible Electronics Technology.....	1
1.1.1 Background of Flexible Technology.....	1
1.2 Flexible Electronics Materials.....	2
1.2.1 Flexible Substrates .....	4
1.2.2 Polyimide (PI) .....	7
1.2.3 Device Layer .....	9
1.3 Fabrication Techniques for Flexible Electronics .....	10
1.3.1 Photolithography Technique .....	11
1.3.2 Scanning Beam Lithography Technique .....	12
1.3.3 Fabrication by Molding And Embossing .....	13
1.3.4 Additive Printing.....	15
1.4 Laser Scribing Technique.....	15
1.5 Supercapacitor (Application) .....	16
<b>Chapter 2: Literature Review .....</b>	<b>17</b>
2.1 Energy Storage .....	17
2.2 Supercapacitors .....	19
2.2.1 Types of Supercapacitors .....	20
2.3 Electrical Double Layer Capacitor (EDLC):.....	21

2.4	Pseudo capacitors .....	22
2.5	Hybrid supercapacitor .....	22
2.5.1	Composite Hybrid .....	23
2.5.2	Asymmetric Hybrid.....	23
2.5.3	Battery Type Hybrid.....	23
2.6	Electrode Materials .....	23
2.6.1	Carbon Materials .....	24
2.6.2	Metal Oxide.....	25
2.6.3	Conducting Polymers .....	26
2.6.4	Composites .....	26
2.7	Fabrication Methods.....	26
2.7.1	Electrode Fabrication Methods .....	26
2.8	Laser Scribing Technology .....	28
2.8.1	Laser Scribing Based on Graphene Oxide .....	30
2.8.2	Laser Scribing Based on Polymers.....	31
2.9	Aims and Objectives .....	31
<b>Chapter 3: Methodology .....</b>		<b>32</b>
3.1	Materials Required .....	32
3.1.1	Polyimide Substrate.....	32
3.1.2	Poly (Vinyl Alcohol) PVA.....	33
3.2	Apparatus for Electrolyte Preparation.....	34
3.3	Instrumentation.....	35
3.3.1	Laser Engraver .....	35
3.3.2	Two Probe Station.....	36
3.3.3	Digital Multimeter (DMM) .....	37
3.4	Electrodes Formation .....	37
3.5	Electrolyte Preparation.....	38
3.5.1	Liquid or Aqueous Electrolytes.....	39
3.5.2	Gel Electrolytes .....	39
3.6	Device Formation.....	41
3.7	Device Packaging.....	42

<b>Chapter 4: Characterization Techniques.....</b>	<b>43</b>
4.1    Fourier Transform Infrared Spectrophotometer .....	43
4.1.1    Instrumentation.....	44
4.2    Raman Spectroscopy .....	45
4.3    X-ray Diffraction analysis .....	46
4.3.1    Instrumentation.....	47
4.4    Scanning Electron Microscope.....	49
4.4.1    Instrumentation.....	50
4.5    Electrochemical Work Station .....	50
<b>Chapter 5: Results and Discussion .....</b>	<b>52</b>
5.1    Material Characterization.....	52
5.1.1    Scanning Electron Microscopy .....	52
5.1.2    X-Ray Diffraction Microscopy .....	53
5.1.3    Raman Spectroscopy .....	53
5.1.4    Fourier Transform Infrared Spectroscopy.....	54
5.2    Laser Engraver Characterization.....	55
5.3    Device Characterization .....	56
5.3.1    I-V characterization.....	56
5.4    Supercapacitor Testing.....	57
5.4.1    Conductivity Test .....	57
5.4.2    Electrochemical Testing of Supercapacitor.....	58
5.4.3    Supercapacitor Stability Test .....	63
5.4.4    Supercapacitor Durability Test.....	63
5.5    Calculations.....	64
<b>Conclusions .....</b>	<b>67</b>
<b>Recommendations .....</b>	<b>68</b>
<b>References .....</b>	<b>69</b>

# List of Figure

Figure 1-1 Different types of flexible substrates: a) Polyimide PI, (foldable and rollable), b) Stainless Steel (permanently deformed able) and c) PDMS (elastically stretchable and bendable .....	3
Figure 1-2 Synthesis of Polyimide (PI). Copyright 2018 by John Wiley and Sons. ....	7
Figure 1-3 Alternate synthesis routes for polyimide. Using a) semiester anhydrides, and b) diacetylated diamines as the reactants respectively. Copyright 2018 by John Wiley and Sons. ....	8
Figure 1-4 Schematic illustrates etching and electroplating conventional pattern transfer techniques .....	10
Figure 1-5 Shows two different photoresists; Positive and negative and how their chemistry changes after exposure to light [4]. ....	11
Figure 1-6 Four different lithography fabrication techniques of flexible electronics with their technical specifications Copyright 2018 by John Wiley and Sons. ....	12
Figure 1-7 Process flow of a roll to roll nanoimprint lithography R2RNIL. Copyright 2018 by John Wiley and Sons. Reprinted with permission .....	14
Figure 1-8 Nanoimprint lithography process and technical specifications. Copyright 2018 by John Wiley and Sons. ....	15
Figure 1-9 A process flow of laser scribing through a DVD burner. Copyright 2018 by The American Association for the Advancement of Science. ....	16
Figure 2-1. Specific Energy Vs Specific Power plot for different energy storage devices, Copyright 2018 by International Journal of Electrochemical science. ....	18
Figure 2-2 Types of Supercapacitor, Copyright 2018 by International Journal of Electrochemical science. ....	21
Figure 2-3 Schematic representation of three types of Supercapacitor: (a) EDLC; (b) Pseudocapacitor; (c) Hybrid Capacitor. Copyright 2018 by American Society of Civil Engineers. ....	22



Figure 2-4 Illustrates the four different steps of Laser scribing i) fabrication ii) patterning iii) device iv)System. Copyright 2018 by the Japan Society of Applied Physics. ....	28
Figure 3-1 Different repeating units of polyimide, Copyright 2018 by The Elsevier Ltd.	33
Figure 3-2 Functionalization of Poly (vinyl Alcohol), Copyright 2018 by Taylor & Francis Group, LLC. ....	34
Figure 3-3 (a) Photograph of laser engraver setup, (b) Software used for laser engraver .....	36
Figure 3-4 (a)Photograph of Digital multimeter (DMM) (b) Resistance measurement of electrodes using DMM, (c) Zoomed image of electrodes.....	37
Figure 3-5 Image of two stack type supercapacitor electrodes.....	38
Figure 3-6 Classification of electrolyte for supercapacitor, Copyright 2018 by the Royal Society of Chemistry.....	38
Figure 3-7 shows the sizes of bare ions, hydrated ions, and ionic conductivity values. Copyrights by 2018 The Royal Society of Chemistry.....	39
Figure 3-8 Phosphoric acid with PVA gel electrolyte synthesis .....	41
Figure 3-9 Schematic diagram of stacked supercapacitor .....	42
Figure 3-10 Packed form of stacked supercapacitor .....	42
Figure 4-1 Mode of vibrations in FTIR Spectroscopy .....	44
Figure 4-2 Schematic diagram of working of FTIR spectrophotometer [1] .....	45
Figure 4-3 Schematic illustration of Raman Spectroscopy .....	46
Figure 4-4 X-ray diffraction by planes of crystal [2] .....	47
Figure 4-5 a) XRD diffractometer in SCME, NUST b) Schematic of XRD .....	49
Figure 4-6 Interaction of electronic beam with matter[2].....	49
Figure 4-7 Schematic Illustration of working of SEM [3] .....	50
Figure 4-8 Schematic diagram of Electrochemical work station.....	51
Figure 4-9 Electrochemical impedance spectroscopy setup.....	51
Figure 5-1 SEM images (a) PI and rPI surface; (b) zoomed image of rPI ; (c) cross sessional view.....	52
Figure 5-2 XRD image of PI and rPI .....	53

Figure 5-3 Raman Spectroscopy of PI and rPI .....	54
Figure 5-4 FTIR image of PI and rPI .....	55
Figure 5-5 a) Laser connections with computer via USB b) The actual laser c) the software laser uses d) Laser scribing over polyimide sheet .....	55
Figure 5-6 a) shows the experiment being conducted at NCP b) Power vs division plot c) Wavelength plot.....	56
Figure 5-7 Conductivity test of PI and rPI .....	58
Figure 5-8 Cyclic Voltammetry graphs of different electrolytes at fixed scan rate of 20mV/s .....	59
Figure 5-9 Cyclic Voltammetry graphs of different electrolytes at Scan Rate of 20mV/s, 50mV/s and 100mV/s.....	60
Figure 5-10 Cyclic Voltammetry graphs of different supercapacitor (electrodes formed at different laser intensity) having Phosphoric acid with PVA electrolyte .....	61
Figure 5-11 Effect of different laser intensity and Scan rate on Capacitance is shown ..	62
Figure 5-12 Cyclic Voltammetry and galvanostatic charge discharge images (a) CV graphs of supercapacitor electrodes fabricated at laser intensity of 138mW, (b)Charge/discharge graphs of respective supercapacitor shown in (a) ,(c) CV graphs of supercapacitor electrodes fabricated at laser intensity of 90mW ,(d) Charge/discharge graphs of respective supercapacitor shown in (c).....	63
Figure 5-13 Supercapacitor durability and efficiency graphs .....	64
Figure 5-14 Supercapacitor having different electrolyte capacitance values at different scan rates. ....	64

## List of Tables

Table 1 Properties of three typical materials for 100- $\mu\text{m}$ -thick foils [13-15]. Copyright 2018 by Springer Nature. ....	4
Table 2 Potential candidates for plastic polymer substrates [18]. Copyright 2018 by Springer Nature. ....	6
Table 3 Properties of 25 $\mu\text{m}$ thick polyimide (PI) films. Copyright 2018 by Elsevier. ....	9
Table 4 Comparison between different electrochemical energy storage technologies, Copyrights 2018 by Elsevier Ltd. ....	18
Table 5 Comparison between supercapacitor and batteries, Copyrights by 2018 Elsevier Ltd. ....	19
Table 6 Different electrode fabrication methods in terms of materials, advantages, and disadvantages. Copyrights 2018 By ASCE ....	27
Table 7 Common substrate materials and application of LSG devices. Copyright 2018 by The Japan Society of Applied Physics. ....	29
Table 8 Reduced PI sample I-V characteristics results. ....	57
Table 9 Literature comparison of capacitance value ....	66

# Abbreviations

Acronym	Meaning
<b>PI</b>	Polyimide
<b>rPI</b>	Reduced Polyimide
<b>GO</b>	Graphene Oxide
<b>LSG</b>	Laser Scribed Graphene
<b>SEM</b>	Scanning Electron Microscopy
<b>XRD</b>	X-Ray Diffraction
<b>FTIR</b>	Fourier Transform Infrared Spectroscopy

# Chapter 1: Introduction

## 1.1 Flexible Electronics Technology

Flexible electronics technology covers a wide range of applications which includes flexible display, flexible solar cell, flexible lighting and many more. Recently, it has been estimated that there are about 1500 worldwide research units working on different aspects of flexible electronics technology. According to market analysis, the estimated revenue of flexible electronics can reach 30 billion USD in 2017 and 300 billion USD by 2028. In Europe the range of research topics included are materials, systems, processes and different applications of flexible electronics. In the US, the research is mostly driven by military applications. Asian companies greatly invest in flexible display [5].

It is common knowledge that the computers or mobile phones consists of a hard-electronic circuit board which is green in color and is mounted with various electronics components like chips, resistors, transistors and capacitors. However, owing to recent advancement in technology, electronics circuit boards are not stiff anymore and have become flexible enough that we can bend or even fold them.

Flexible electronics technology is trending now-a-days for two main reasons:

1. It promises a completely new design tool. For example, imagine a small smartphone that can be easily wrapped around our wrists or a large flexible television that is foldable.
2. It is cost effective. Fabrication technology mostly require very complex processes which costs multi-billion-dollars for foundries. Researchers are trying to print flexible electronics on plastics films in the same way as we are printing ink on newspapers.

### 1.1.1 Background of Flexible Technology

Flexible technology has an extensive background. Thin things are flexible in nature. Forty years before, silicon solar cells were thinned to increase their power ratio so that we can use them in satellites. Now a days, silicon-integrated circuits are thinned it is difficult to break easily even when someone sits on these boards. Flexible materials can be of different

qualities, like bendable, elastic, lightweight, conformally shaped or large area. This technology has opened its different boundaries, these boundaries moving quickly towards development and application. If we talk about industrial public, flexible technology meaning is flexible displays like LED or TV screens and X-ray array sensors [6]. For researchers this technology meaning is conformally shaped displays, flexible sensors, flexible textiles electronics and electronic skin. The first flexible thin-film transistor (TFT) was fabricated in 1968, this was done by Brody and his colleagues when they made a TFT of tellurium on a thin paper strip and planned that TFT will use for display purposes [7]. During these years, Brody's group made TFTs on many different flexible substrates, which includes Mylar, polyethylene and aluminum wrapping foil. We can bent TFTs to a 1/16" radius and it has continued to function well [8].

In the 1980s, the active-matrix liquid-crystal display (AMLCD) industry was started in Japan by adopting the machines of large-area plasma enhanced chemical vapor deposition (PECVD) that had been developed for the fabrication of a Si:H solar cell.

## **1.2 Flexible Electronics Materials**

Generally large-area flexible electronics structure is made up of

1. Substrate material
2. Backplane electronics
3. Front-plane electronics
4. Device Encapsulation

For making flexible devices, all components comply with bending to some degree and work properly without changing their functions. Two basic techniques commonly used for the fabrication of flexible electronics are:

- ❖ Transfer and bonding of finalized circuits on a flexible material
- ❖ Direct fabrication of electronic circuits on flexible substrate

In many applications, the majority of the surface will be covered with electronics fabricated directly on the substrate. There are many approaches to integrating disparate materials and oftentimes flexible substrates are not fully compatible with existing planar silicon microfabrication processes. Direct fabrication may require (1) relying on polycrystalline or amorphous semiconductors because these can be grown on foreign

substrates, (2) developing new process techniques, (3) introducing new materials, and (4) striking a compromise between device performance and low process temperatures tolerated by polymer foil substrates. Direct fabrication techniques for flexible electronics applications is currently the rage amongst researchers. Other than this, latest process techniques include mask printing [9], active device materials additive printing [10, 11] and the introduction of different electronics functions by using native chemical reactions[12]. Flexibility can be defined in many ways according to the manufacturers and users required flexible properties. As a mechanical characteristic, flexibility is classified into three main categories as shown in Figure 1.1:

- ❖ Bendable or Roll able
- ❖ Permanently shaped
- ❖ Elastically stretchable

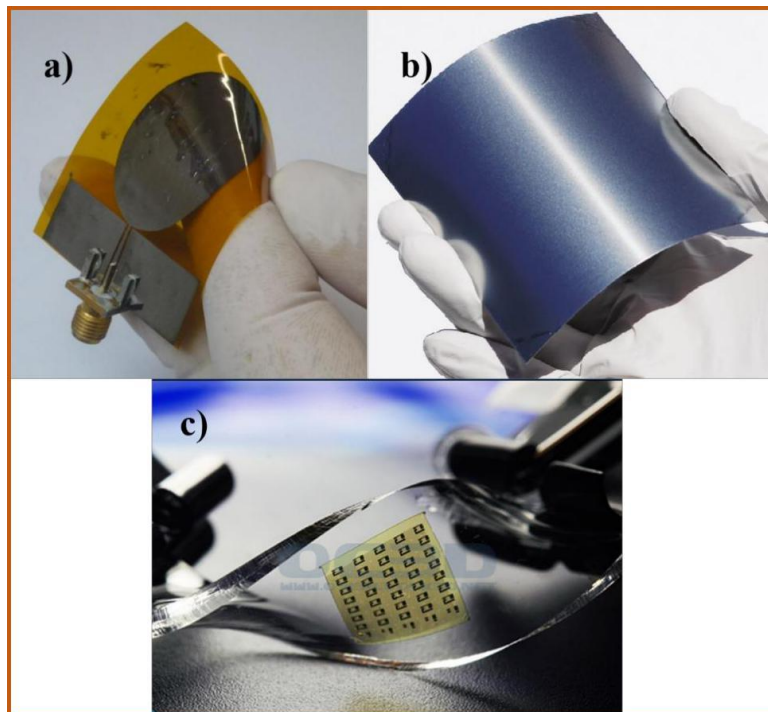


*Figure 1-1 Different types of flexible substrates: a) Polyimide PI, (foldable and rollable), b) Stainless Steel (permanently deformed able) and c) PDMS (elastically stretchable and bendable)*

The apparatus for flexible microfabrication have been made for mostly flat substrates. Therefore, these days all manufacturing is done on flat workpiece that is shaped only as

late as possible during the process. This approach benefits from the many technology based established by the planar integrated circuits and display industries.

### 1.2.1 Flexible Substrates

Three different types of materials are used as substrate, for the application of flexible electronics are:

1. Metals
2. Organic polymers (plastics)
3. Flexible glass

Properties of these materials are listed in Table 1 for 100- $\mu\text{m}$ -thick foils.

*Table 1 Properties of three typical materials for 100- $\mu\text{m}$ -thick foils [13-15]. Copyright 2018 by Springer Nature.*

Property	Unit	Stainless Steel (430)	Glass (1737)	Plastics (PI, PEN)
Thickness	$\mu\text{m}$	100	100	100
Weight	$\text{g}/\text{m}^2$	800	250	120
Roll-to-roll processable?	–	Yes	Unlikely	Likely
Safe bending radius	$\text{cm}$	4	40	4
Visually transparent?	–	No	Yes	Some
Elastic modulus	$\text{GPa}$	200	70	5
Maximum process Temperature	$^{\circ}\text{C}$	1,000	600	180, 300
CTE	$\text{ppm}/^{\circ}\text{C}$	10	4	16
Permeable to oxygen, water vapor		No	No	Yes
Prebake required?	–	No	Maybe	Yes
Buffer layer required? Why?	–	yes: electrical insulator, chemical passivation	Maybe	yes: adhesion, chemical passivation
Electrical conductivity	–	High	None	None
Thermal conductivity	$\text{W}/\text{m}\cdot^{\circ}\text{C}$	16	1	0.1–0.2
Deform after device Fabrication	–	No	No	Yes
Planarization required?	–	Yes	No	No

#### 1.2.1.1 Thin Flexible Metal Foil

Metallic foil having a thickness less than 125 $\mu\text{m}$  are flexible substrates and are prospective substrates for the applications of reflective or emissive displays, because they do not



require transparent displays. Stainless steel is usually used for its chemical robustness as it is highly resistant to corrosion and other chemical processes. Stainless steel can withstand a processing temperature of 1000°C and is dimensionally stable. It is impermeable to water and oxygen, can work as a heat sink and can show electromagnetic shielding as well.

#### *1.2.1.2 Thin Flexible Glass*

Thin flexible glass plates are commercially being used as the substrate material for flat-panel displays. These glass become flexible substrate around the thickness of ~100µm [16]. Flexible glass foils have been obtained by using the down-draw method for its manufacturing by which around 30µm thickness can be achieved. All the qualities of a flexible glass are retained such as smooth surface of average roughness ~ 1nm or less, temperature around 600°C, ultra-high optical transmittance in the visible spectrum and very low coefficient of thermal expansion which is (CTE) ~  $4 \times 10^{-6}$  per °C. On the other hand, flexible glass plate is extremely delicate and prone to crack propagation. There are three strategies used to remediate these problems

1. Applying a thin hard coat
2. Coating with a thick layer of polymer
3. Using a plastic foil to laminate the glass.

#### *1.2.1.3 Flexible Plastic Films*

Polymeric plastic foils are inexpensive, flexible and permit roll-to-roll or direct writing. They are simply permeated by oxygen and water. However, polymer plastic substrates lack dimensional stability and a low CTE. As the polymer undergoes heating and cooling cycles, they shrink in size and their sizes do not remain the same. To solve the problem of shrinkage they need to be annealed for a longer time period [17]. A small mismatch of CTE or temperature during processing between the substrate and inorganic device materials can make a free-standing device, whereas a large difference can break the device layer. Therefore, polymers with CTE less than 20 ppm/°C can be preferred as substrate materials for silicon based devices [14].

Table 2 Potential candidates for plastic polymer substrates [18]. Copyright 2018 by Springer Nature.

Properties	PET	PEN	PC	PES	PI
	Melinex	Teonex	Lexan	Sumilite	Kapton
T <sub>g</sub> , °C	78	121	150	223	410
CTE (-55 to 85°C), ppm/°C	15	13	60–70	54	30–60
Transmission (400–700 nm), %	89	87	90	90	Yellow
Moisture absorption, %	0.14	0.14	0.4	1.4	1.8
Young's modulus, Gpa	5.3	6.1	1.7	2.2	2.5
Tensile strength, Mpa	225	275	–	83	231
Density, gcm <sup>-3</sup>	1.4	1.36	1.2	1.37	1.43
Refractive index	1.66	1.5–1.75	1.58	1.66	–
Birefringence, nm	46	–	14	13	–

There are following potential polymers as shown in the Table 2 [18] for such applications include,

1. Semi-crystalline thermoplastic polymers e.g. polyethylene terephthalate (PET) and polyethylene naphthalate (PEN)
2. Amorphous thermoplastic polymers e.g. polycarbonate (PC) and polyethersulphone (PES)
3. High glass transition (T<sub>g</sub>) materials such as polyarylates (PAR), poly-cyclic olefin (PCO), and **polyimide (PI)**

Although PCO, PAR, PES and PC have high T<sub>g</sub> their CTE(s) are around 50 ppm/ °C and have very poor resistance to chemical processes. PET, PEN and **PI** have relatively low CTEs of 15, 13, and 16 ppm/ °C, respectively, and a high inertness to chemical processes. PET and PEN are transparent in nature and absorb very little water (~0.14%) but their service temperatures are ~150 and ~200 °C respectively, even after their thermal annealing. On the other hand, **PI** has a high T<sub>g</sub> of approximately 350 °C and has a yellow color as it absorbs blue light and can absorb water up to 1.8%. The permeation rates for oxygen and water in polymers are 1-10 g/m<sup>2</sup>/day and 1-10 cm<sup>3</sup>/m<sup>2</sup>/day and permitted range is approximately 10<sup>-6</sup> g/m<sup>2</sup>/day and 10<sup>-5</sup> cm<sup>3</sup>/m<sup>2</sup>/day [19].

## 1.2.2 Polyimide (PI)

Polyimides (PI) are a class of polymers which are heteroaromatic and thermally very stable. Polyimides are one of the polymers which are resistant to heat. They can be used as flexible films, foams, adhesives, plastic moldings, resin matrices for composites materials and wire coating for enamels[20].

### 1.2.2.1 Production of Polyimides (PI)

Most practical way for synthesis of polyimides involves condensation reactions[21]. This synthesis process takes place at a low temperature of 50 °C. Polycondensation reaction of aromatic anhydride takes place in a polar solvent (e.g. dimethylacetamide) to form polyamic acids. This is a soluble and fusible intermediate which can be change into fibers, flexible films or impregnated fibrous reinforcements, which are converted into cyclic polyimides(PI) either by heating them (200 – 300 C° [22-24] or through chemical changes[25] e.g. as shown in Figure 1.2, carboxylic anhydrides in the presence of tertiary amine catalysts was as dehydrating agents.

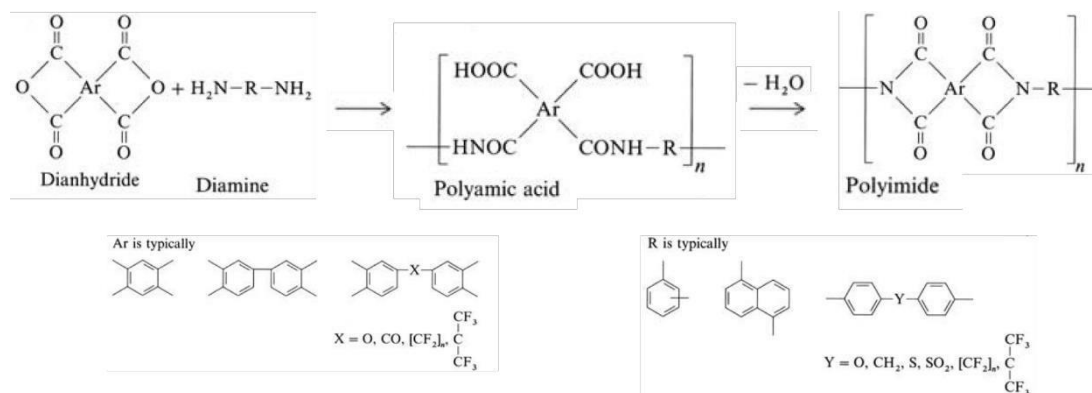


Figure 1-2 Synthesis of Polyimide (PI). Copyright 2018 by John Wiley and Sons.

For making films and fibers as the finished product, it is paramount for the polyamic acid (intermediate) to be of a very high molecular mass, purity, stoichiometry and the mixing order of reactants[26]. The main problem is the instability of polyamic acid and the volatile by-products formed such as water, methanol or acetic acid. Due to the instability, the polymeric acid must be stored in completely dry and refrigerated conditions. Evolution of by-products such as production of water presents some of their own difficulties for which more hydrolysis must be done. These problems are improved by modifying the synthesis routes as shown in Figure 1.3. Using semi-esters of anhydrides and or diacetylated

diamines confirms that an alcohol or acetic acid will be produced during the imidization process.

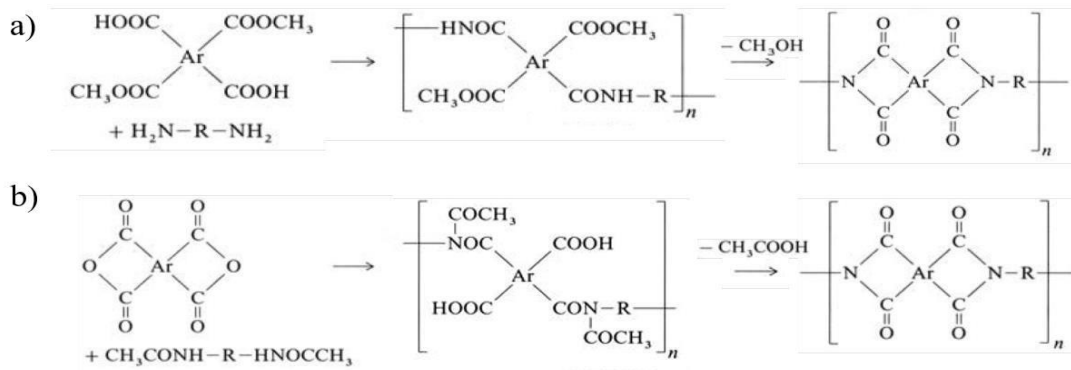


Figure 1-3 Alternate synthesis routes for polyimide. Using a) semiester anhydrides, and b) diacetylated diamines as the reactants respectively. Copyright 2018 by John Wiley and Sons.

### 1.2.2.2 Synthesis of Polyimide (PI) Films

Polyimide films are generally synthesized by solution casting method. In this method a solution of polyamic precursor is deposited on a substrate and then it is converted in to polyimide (PI) by the action of excessive heat of 300 °C or through chemical reactions [27]. Another method for casting polyimide (PI) films is through phenolic solvents. A polyamic acid derived from the reaction of ODA (4,4'-diaminodiphenylether) and BPDA (3,3',4,4'-biphenyltetracarboxylic dianhydride) well-known as ODA-BPDA. This is casted onto a substrate from its p-chlorophenol solvent, and then heated at 300 °C for the imidization and driving away of the solvent. ODA precursor is used by Ube Industries as known as Upilex R. Similar methods are used to cast a very famous product such as Kapton® commercially.

### 1.2.2.3 Properties of Polyimide (PI)

The properties of Kapton®, Upilex® R and S are described in Table 3. Kapton is manufactured in Du Pont a USA based company whereas Upilex is manufactured by Ube industries which is based in Japan and are marketed by ICI. When we compare Kapton® and Upilex R® in terms of their properties, both carry the same diamine (ODA), but they have a significant difference between their Tg, 385° and 285° respectively. However, they can be compared in terms of their mechanical and electrical properties. Upilex R® has a lower water, 250 °C shrinkage and good hydrolytic resistance. There is a sharp difference

between Kapton® and Upilex S®. As far as we compare the mechanical properties of both polyimides, Upilex S® is stiffer than Kapton®, while having a lower percentage of elongation making Upilex S® more brittle than Kapton®.

Table 3 Properties of 25µm thick polyimide (PI) films. Copyright 2018 by Elsevier.

Property	Kapton®	Upilex R®	Upilex S®
<b>Physical Properties</b>	<b>25°C</b>	<b>23°C</b>	<b>23°C</b>
<b>Tensile strength, MPa</b>	172	172	276
<b>Stress at 5% elongation, MPa</b>	90	83	180
<b>Ultimate elongation %</b>	70	130	30
<b>Tensile modulus, GPa</b>	3	2.6	6.2
<b>Density g/cm<sup>3</sup></b>	1.42	1.38	1.47
<b>Electrical Properties</b>	<b>25°C</b>	<b>25°C</b>	<b>25°C</b>
<b>Volume resistivity (ohm-cm)</b>	10 <sup>18</sup>	10 <sup>17</sup>	10 <sup>17</sup>
<b>Dielectric constant (10<sup>3</sup> Hz)</b>	3.5	3.5	3.5
<b>Dissipation factor (10<sup>3</sup> Hz)</b>	0.003	0.0014	0.0013
<b>Dielectric strength (kV/mm)</b>	7000	280	286
<b>Thermal properties</b>			
<b>Glass transition temperature (°C)</b>	385	285	>500°C
<b>Coefficient of thermal expansion (m/m/°C)</b>	2.0 × 10 <sup>-5</sup>	1.5 × 10 <sup>-5</sup>	0.8 × 10 <sup>-5</sup>
<b>Oxygen index (%)</b>	37	55	66
<b>Shrinkage % (250°/30min)</b>	0.3	0.18 for 2hr	0.18 for 2hr
<b>Chemical properties</b>			
<b>Hygroscopic coefficient expansion (cm/cm/% RH) 20-80% RH x 10<sup>-5</sup>)</b>	2.2	2	1
<b>Solvent Resistance</b>	Excellent	Excellent	Excellent
<b>Gas Permeability</b>	23°C	20°C/24 hr. (g/m <sup>2</sup> /mm)	
	kg/m <sup>2</sup> /day/ (MPa/m m)		
<b>Water vapor</b>	0.021	0.56	0.043
	23°C	30°C (ml/m <sup>2</sup> /mm)	
	(1/m <sup>2</sup> /day/ (MPa/m m)		
<b>He</b>	1.61	55.9	-
<b>N<sub>2</sub></b>	0.023	0.76	-
<b>O<sub>2</sub></b>	0.021	2.54	0.02
<b>CO<sub>2</sub></b>	0.174	2.92	0.03

### 1.2.3 Device Layer

Graphene and graphene like materials get great scientific and researcher attention because of its rare and very attractive properties for use in many applications like electronics,

medicine, photovoltaics and composites. Graphene, and its derivatives, have shown great potential to various applications because it has high surface-to-volume ratio, very low noise. It is very sensitive to electronics properties as changes occur in its surrounding. Particularly, the composites of graphene with polymers show a very high potential towards flexible electronics technology. The common examples of graphene based flexible electronics applications are pressure sensor, artificial skin, supercapacitors and wearable electronics. Graphene based materials have high surface to volume ratio due to which it has the capability to store more charge on its surface, because of this property it is commonly used for the charge storage applications. These materials have the advantages like ease and low cost of fabrication, as well as the simple way of conversion and readout mechanism, due to which these are widely used.

### 1.3 Fabrication Techniques for Flexible Electronics

Micro-fabrication term is given to the process of fabricating structures and devices with dimension of micrometer or smaller. The motivation for doing this miniaturization of structure is to,

- ❖ Lower device cost,
- ❖ Increase the surface density of components,
- ❖ Increase the performance of device and integrated circuits.

Method for the fabrication of nano electronics is photolithography and particle beam lithography. Figure 1.4. Shows the steps for a conventional lithographical process takes place to fabricate a device or structure. A photoresist is spin on the quartz crystal and goes through several processes such as exposure to light and afterwards to transfer the pattern on the device layer or on the substrate [28].

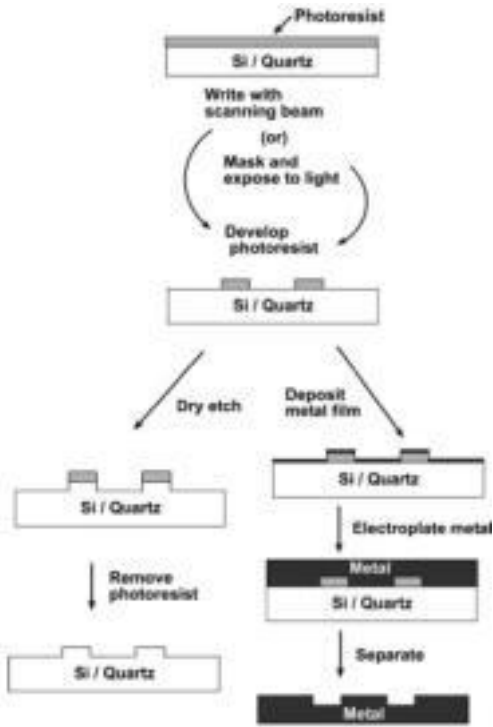


Figure 1-4 Schematic illustrates etching and electroplating conventional pattern transfer techniques

### 1.3.1 Photolithography Technique

In photolithography process, the photoresist layer is applied on to the substrate, after that it is exposed to light using a photomask, which has a separate pattern on it and it projects on to the resist below. The resist material is of two different types, positive photoresist or negative photoresist. After exposure to light, the resist might undergo some changes either the exposed region will increase in solubility or may it become less soluble depending on the chemistry of the photo resist as shown in Figure 1.5.

Some most commonly used photoresists materials are Parylene C, SU-8 and **polyimide (PI)** [29]. The patterned resist act as template for the formation of IC on the silicon substrate followed by etching of silicon and then finally removal of the photoresist. This is the parallel type lithography; all the layers are patterned in the single exposure to light. Hence for the formation of multiple layer either the steps need to be repeated or post processing have to be done. The required set-up for multilayer is very expensive, but it is highly optimized to perform at throughputs of 100 wafer per hour and more ( $28 \text{ m}^2 \text{ hr}^{-1}$ )[30].

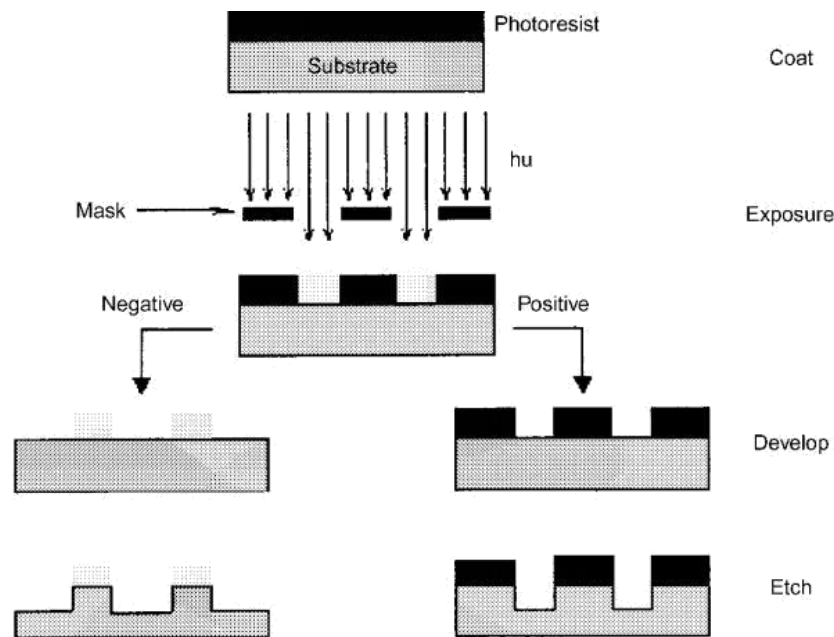


Figure 1-5 Shows two different photoresists; Positive and negative and how their chemistry changes after exposure to light [4].

### 1.3.2 Scanning Beam Lithography Technique

SBL is a direct-writing lithographic technique. A pattern is written on to the photoresist by manipulation beams such as electrons, photons, or ions. For the fabrication of photo-masks this method is primarily used. Figure 1.6 describe four more commonly used fabrications techniques for synthesizing flexible electronics.

Fabrication method	Material complexity	Resolution	Total size	Geometric diversity	Materials diversity	Throughput
 <p>Photolithography</p>	Multiple materials possible	Down to 37 nm/315 potentially sub-10 nm/315	15 cm diameter circular substrates	Two tunable dimensions	Only photosensitive materials	Very high
 <p>Scanning beam lithography: Optical beam lithography (OBL)</p>	Single material structures	52 nm/315	2 x 2 cm <sup>2</sup> substrates/315	Three tunable dimensions	Only photosensitive materials	Low
 <p>Scanning beam lithography: Ion beam lithography (IBL)</p>	Single material structures	8 nm/315	12.5 x 12.5 mm <sup>2</sup> pillar arrays/315 continuous-sized patterns/315	Two tunable dimensions	Polymeric or metallic materials	Low
 <p>Scanning beam lithography: Electron beam lithography (EBL)</p>	Single material structures	4 nm/315	Wafers and photoresists up to around 30 cm diameter/315	Two tunable dimensions	Polymeric or metallic materials	Low

Figure 1-6 Four different lithography fabrication techniques of flexible electronics with their technical specifications Copyright 2018 by John Wiley and Sons.



#### *1.3.2.1 Optical Beam Lithography Technique*

OBL is a mask less photolithography capable of producing 2D structures with well-defined height as well as depth. By using UV light as a source, photons react with the surface of the substrate material rendering the resist to be more or less soluble [28]. As the height of the structures can also be controlled by varying the intensity and the focal point of the optical beam, 2D structured are projected onto the photoresist and then finally on the substrate.

#### *1.3.2.2 Electron Beam Lithography Technique*

In EBL, electrons are accelerated on the resist surface on to the substrate, the beam electrons interact with electrons present in the resist resulting the crosslinking or chain scission of its polymeric chains [29]. Some common resist materials that are commonly used are poly (methyl methacrylate) (PMMA), hydrogen silsesquioxane (HSQ), NaCl, ZEP, SiO<sub>2</sub> or LiF [30]. The resolution is not determined by the diameter of the electron beam as well as the mechanical resistance of the resist material during the development step. For getting the high resolution, a lower electron dose is used; therefore, the throughput is significantly low [31].

#### *1.3.2.3 Ion Beam Lithography Technique*

Focused ion beam is used to change the surface structure, chemistry or simply removal of atoms. An advantage of IBL over EBL is that the ions used are heavier than electrons hence less scattering occur due to which the chances of proximity effect decreases. As the ions are heavier than electrons they have a larger impact on the surface of the substrate so that even the lower dose of ions leaves a pattern. In IBL there is no need of resist; however it is slower technique.

### **1.3.3 Fabrication by Molding And Embossing**

In these techniques a 3D template is used to press a pattern on to the resist layer which pasted on to the substrate. In hot embossing the resist is heated before the template being pressed [32]. These molds are usually composed of silica or quartz as they are inert to most of the pre-polymers and monomers, and they are fabricated by SPL [33]. Due to low CTE of quartz and silica they can be used at higher temperatures. By using imprinting method, we can get the through-put pretty high because the imprint thickness is freely tune

able. The through-put is around  $10^{-4} \text{ m}^2 \text{ h}^{-1}$ , this is greater than any serial writing (SPL) technique [34].

### 1.3.3.1 Nanoimprint Lithography Technique

For shaping a polymer glass into desired structure, a mold is used, when it is subjected to heat above its  $T_g$ . During cooling the polymer hardens and the template is removed from it and a pattern on the resist left. This method has extremely small feature sizes about 10nm [35]. For increasing the through put of NIL a technique is used which is known as roll to roll nanoimprint lithography [34].

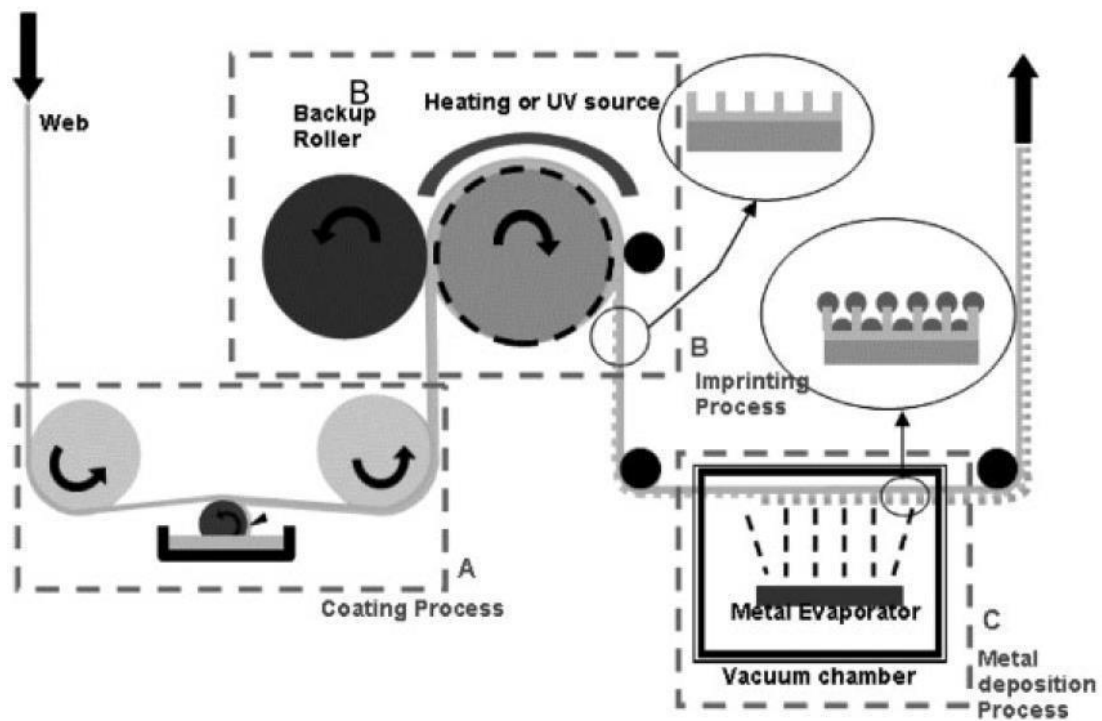


Figure 1-7 Process flow of a roll to roll nanoimprint lithography R2RNIL. Copyright 2018 by John Wiley and Sons. Reprinted with permission

### 1.3.3.1 Step and Flash Imprint Lithography Technique

A photosensitive pre-polymer is used in the molding process of this technique, this pre-polymer polymerizes when UV light source is incident on it. For this the mold used to be transparent to UV light so it can reach the surface of pre-polymer. For this purpose the quartz and silica are best choice as molds. The mold polymerizes when the UV light source is incident on it. This lithography is more suitable for synthesizing multiple stacked layers.

A 4nm width thin line were produced using a PDMS-based UV resist when an ion beam fabricated pattern of HSQ was printed[31].

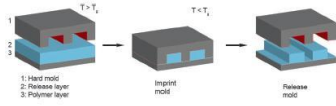
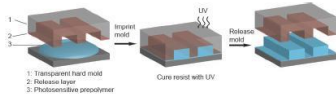
Fabrication methods	Material complexity	Resolution	Total size	Geometric diversity	Material diversity	Throughput
<p>Hard molding: Nanoimprint lithography (NIL)</p> 	Single material structures	30 nm <sup>[35]</sup>	300 × 400 mm <sup>2</sup> <sup>[84]</sup>	One tunable dimension	Only polymeric materials	High
<p>Hard molding: Step-and-flash imprint lithography (SFIL)</p> 	Single material structures	5 nm <sup>[24]</sup>	Up to 250 × 250 mm <sup>2</sup> wafers <sup>[185]</sup>	One tunable dimension	Only polymeric materials	High

Figure 1-8 Nanoimprint lithography process and technical specifications. Copyright 2018 by John Wiley and Sons.

### 1.3.4 Additive Printing

Additive printing can be used for flexible electronics, this will reduce the cost of per square meter[32]. Additive printing is compatible with roll to roll printing, hence this technique also increases the through-put of the process. It does not require vacuum and it uses the device material efficiently without any wastage. All types of materials can be printed such as noble-metal conductors, organic conductors, semiconductors and even insulators. Some organics materials were used to print TFTs [33, 34]. Masks for etching and lift-offs patterns uses inorganics materials [35] and they were printed [36, 37].

## 1.4 Laser Scribing Technique

Laser scribing is another fabrication technique in which limited types of materials such as graphene oxide, polyimide, polyetherimide etc can be used. Laser irradiation is utilized in this method to change the composition and morphology of aforementioned structures. In this process a photothermal reduction takes place due to which certain functional groups are removed from the surface of the material and making surface to be conductive.

This is a very cost-effective fabrication method with minimal chemical loss which makes it environmental-friendly as well. This method is similar to Direct Laser Writing technique but instead of using a pre-polymer and then its polymerizing, in this method we simply reduce the thin films or substrate materials like polyimide (PI).

This fabrication technique has many advantages as follow:

- ❖ Fast and less time-consuming method
- ❖ One step synthesis is done
- ❖ It is environment friendly (No loss of chemicals)
- ❖ Cost effective method

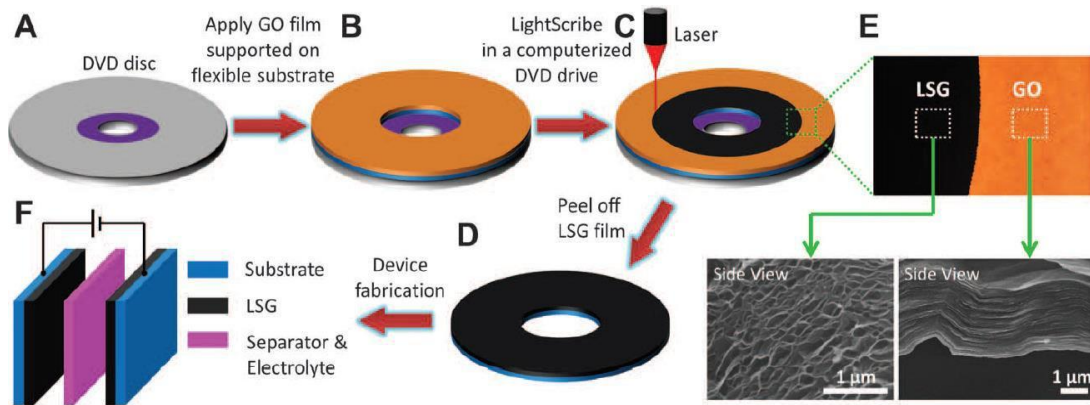


Figure 1-9 A process flow of laser scribing through a DVD burner. Copyright 2018 by The American Association for the Advancement of Science.

## 1.5 Supercapacitor (Application)

Supercapacitor is a device in which electrolyte is sandwiched between the two electrodes. These electrodes are mostly formed of graphene and graphene like material, which have yielded favorable results in terms of high power density and long cycling life. This is a high energy storage device. It has the ability to store energy and it has high-power density and long cycling life. Supercapacitors are expected to impact consumer electronics, electrical power grids, transport and military applications, and various types of electrical instruments for commercial and industrial uses. Further detail of supercapacitor is discussed in next chapter.

## Chapter 2: Literature Review

### 2.1 Energy Storage

Electrochemical energy storage is realized by ion and electrons conductivity and their diffusion in electrodes. The two main devices for storage of electrochemical energy are batteries and supercapacitors. These are the kinds of devices in which electricity is stored by electrochemical process. The electrochemical devices have an anode, a cathode, an electrolyte and a separator. For doing charging an external voltage applied to the electrodes which start the movements of reactions and electrons at the electrodes, during discharge at electrodes electrochemical reactions occur, which generates electrons that flow in external circuit. There are different types of supercapacitors, the principle mechanisms of supercapacitors are electrical double layer and pseudo-capacitive charge storage. Similar to physical dielectric capacitor, a supercapacitor is based on the separation of charges at the interface between an electrolyte and at electrodes. Carbon, transition metal oxides and conducting polymers are commonly used electrode materials for supercapacitors. Electrochemical energy storage show high efficiency, flexibility and versatility among many other energy storage techniques. Supercapacitors have attracted attention due to high power storage capability and it is very desirable for electric vehicles and hybrid electric vehicles applications [38]. The main electrochemical energy storage technologies and their comparison is shown in **Table 3** [39] and **Table 4** [40] show the comparison between supercapacitor and batteries.

How much energy store by a device and its working depends on the properties of material that is used in it. Recently the topic of interest in advanced materials are nanostructured materials because they have unusual mechanical, optical and electrical properties. Materials with reduced dimensions are consider are used in microelectronics. These are now important materials for energy storage [41]. Energy storage devices have attracted more and more interest due to increase demand of mini and portable electronics devices[42] . Batteries have high energy densities, but their power densities are not very high for certain applications where high power and rapid discharge required. Supercapacitor is used as an alternative device for the electrical energy storage, which have high power densities, fast charge/discharge cycles, long cyclic life as compared to

the batteries[39].Therefore research and development of supercapacitor on micro and nanoscale is of great interest [43].

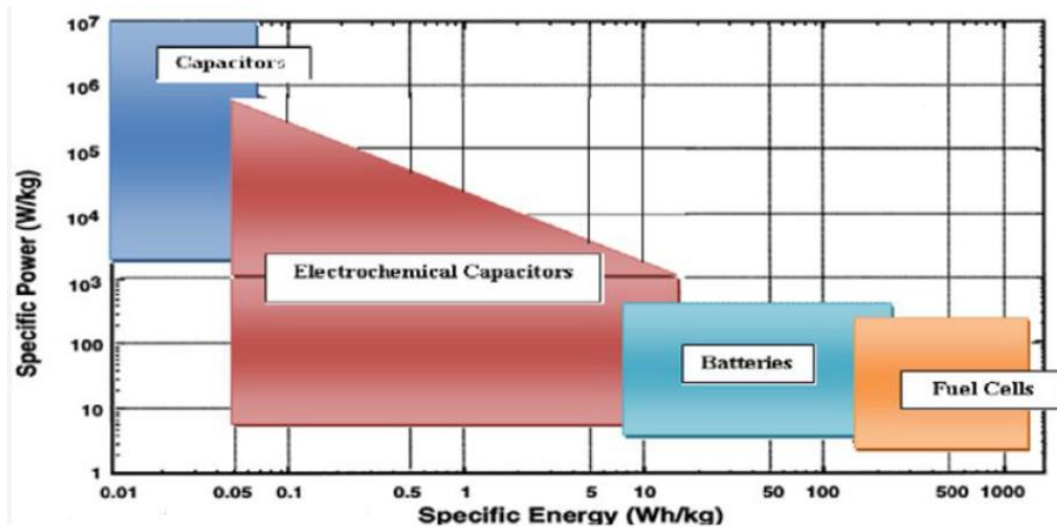


Figure 2-1. Specific Energy Vs Specific Power plot for different energy storage devices, Copyright 2018 by International Journal of Electrochemical science.

Table 4 Comparison between different electrochemical energy storage technologies, Copyrights 2018 by Elsevier Ltd.

Characteristics	Capacitor	Supercapacitor	Battery
Specific energy(Whkg <sup>-1</sup> )	< 0.1	1–10	10–100
Specific power(Whkg <sup>-1</sup> )	>10,000	500-10,000	< 1000
Discharge time	10 <sup>-6</sup> -10 <sup>-3</sup>	s to min	0.3-3h
Charge time	10 <sup>-6</sup> -10 <sup>-3</sup>	s to min	1-5h
Coulombic efficiency (%)	About 100	85-98	70-85
Cycle-life	Almost infinite	>500,000	About 1000

Table 5 Comparison between supercapacitor and batteries, Copyrights by 2018 Elsevier Ltd.

<i>Comparison parameter</i>	<i>Battery</i>	<i>Supercapacitor</i>
<b>Storage mechanism</b>	Chemical	Physical
<b>Power limitation</b>	Reaction kinetics, mass transport	Electrolyte conductivity
<b>Energy storage</b>	High (bulk)	Limited (surface area)
<b>Charge rate</b>	Kinetically limited High,	same as discharge
<b>Cycle life Limitations,</b>	Mechanical stability, chemical reversibility	Side reactions

## 2.2 Supercapacitors

The development of advanced technologies and miniaturized electronic devices required energy of appropriate size, which can be rechargeable. In late 1990s Li and Li-ion batteries were discovered for energy storage. The micro-batteries are used for the harvested energy storage, but major issue with these batteries is their finite life time as maintenance or replacement is not possible in case of permanent structures e.g. in Radio frequency identification (RFID) tags and biomedical implants. The other name of electrochemical capacitors (ECs) is **supercapacitors**, they store energy at the interface between the porous electrode and an electrolyte by the accumulation of ions. The mechanism to store charges is mostly capacitive, during its charge/discharge process no chemical modification of electrode take place, due to which they can provide fast charge/discharge rates, high power and sustain millions of cycles having reasonable power density. Micro scale ECs could satisfy a variety of micro-power demands and it can replace the micro-batteries in electrical energy storage applications where high power delivery is required in very short times[44].

With the rapid growth in technology and increase in energy consumption, the need for new energy resources and efficient way of their storage is becoming critical. Energy storage and its efficient use is the topic of great research interest.

In ancient times for energy storage purpose wood and charcoal were used. About 900 years ago, coal obtained from buried plants were used to store solar energy at much higher density than wood or charcoal. Coal can also be used for fuel. In the 8<sup>th</sup> century it was used in power steam engines and then to produce electricity. Petroleum is another high-density energy storage medium used for solar energy.

Petroleum is not only used as fuel in vehicles but also used to make fibers, plastics and many other things of modern lives. Coal, natural gas and Oil are the main energy sources they are naturally collected and store solar energy. Generators and electric motors were created in the 1870s, after this electric energy become the secondary energy source and primary form of expended energy.

Electricity can be generated via solar power, wind power, nuclear power, hydropower and biogas systems. It is used in almost everything of our lives like lighting, transportation and communication. With the rapid and advanced development of modern technologies and industries and increase of global population, the rate of electrical energy consumption increased. Due to high energy demands, energy storage become more important and desirable, and energy storage techniques are required to enable the efficient and versatile use of energy. In energy storage process, one form of energy is converted into the other form of energy that can be stored and can be converted for use when required. There are many energy storage systems developed to properly use energy and its storage from different energy sources [45].

### **2.2.1 Types of Supercapacitors**

The principle of operation of supercapacitor is based on energy storage and distribution of the ions coming from the electrolyte to surface area of the electrodes. Based on the energy storage mechanism supercapacitors are classified into three classes: Electrochemical



double-layer capacitors, pseudo capacitors, and hybrid supercapacitors as shown in Figure 2.3. We can classify supercapacitors into following types as shown in the Figure 2.2.

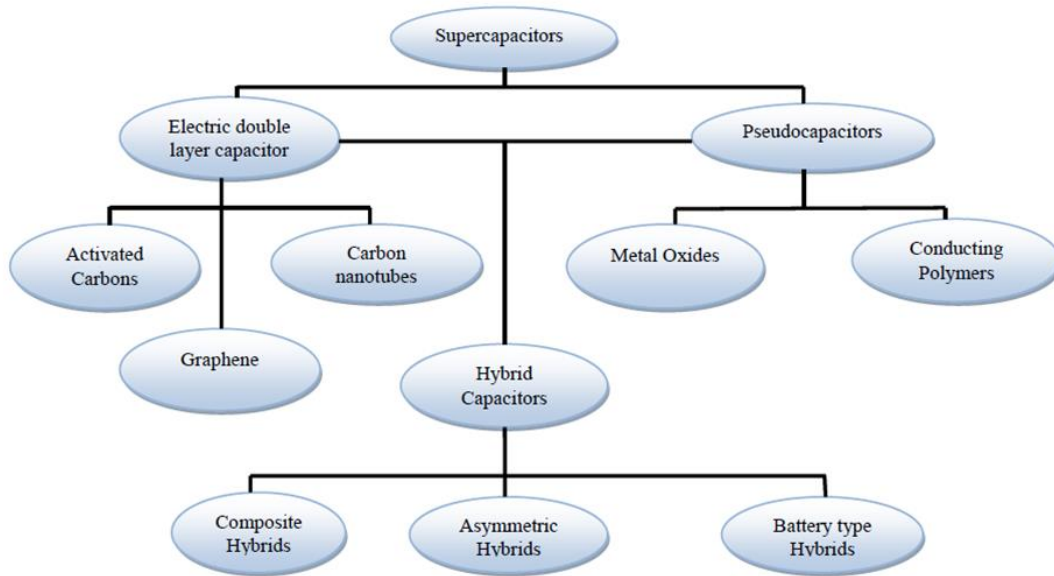


Figure 2-2 Types of Supercapacitor, Copyright 2018 by International Journal of Electrochemical science.

### 2.3 Electrical Double Layer Capacitor (EDLC):

In EDLCs energy storage mechanism is based on the charge separation at the interface formed between an electrolyte and an electrode. In this charge storage mechanism chemical oxidation-reduction (redox) and faradaic reactions are not involved[46, 47]. In EDLCs only physical charge transformation take place due to which they have long cyclic lives. EDLCs have higher energy density because in it the double layer, combined with the increase in surface area and distances between electrodes decreased [48, 49].

The differences between EDLCs and batteries are as follow:

1. EDLCs can withstand millions of cycles but batteries can work best for few thousand cycles.
2. In EDLCS Charge storage mechanism does not involve electrolyte solvent but in Li-ion batteries it contributes to electrolyte inter phase when graphite anode or high-potential cathodes are used[50].

## 2.4 Pseudo capacitors

Pseudo capacitors mechanism is based on faradic redox reactions, its electrode materials are based on conductive polymers, metal oxides or metal doped carbons. When a potential is applied to a pseudocapacitor reduction and oxidation takes place on the electrode material, which involves the passage of charge across the double layer, resulting in faradic current passing through the supercapacitor cell. The faradic process involved in pseudocapacitors allows them to achieve greater specific capacitance and energy densities compared to EDLCs. These supercapacitors have higher energy density due to electrode material. These supercapacitors have higher energy density as compare of electrochemical double layer capacitors but there cyclic lives are shorter[51, 52].

## 2.5 Hybrid supercapacitor

These supercapacitors incorporate mechanism from both pseudo capacitors and EDLCs. A supercapacitor consists of two electrodes separated by a semipermeable membrane which act as a separator to isolate from electrical contact. An electrolyte solution impregnated on the electrodes and separator, which enables the flow of ions between electrodes and prevent electronic current from discharging the cell [53, 54].

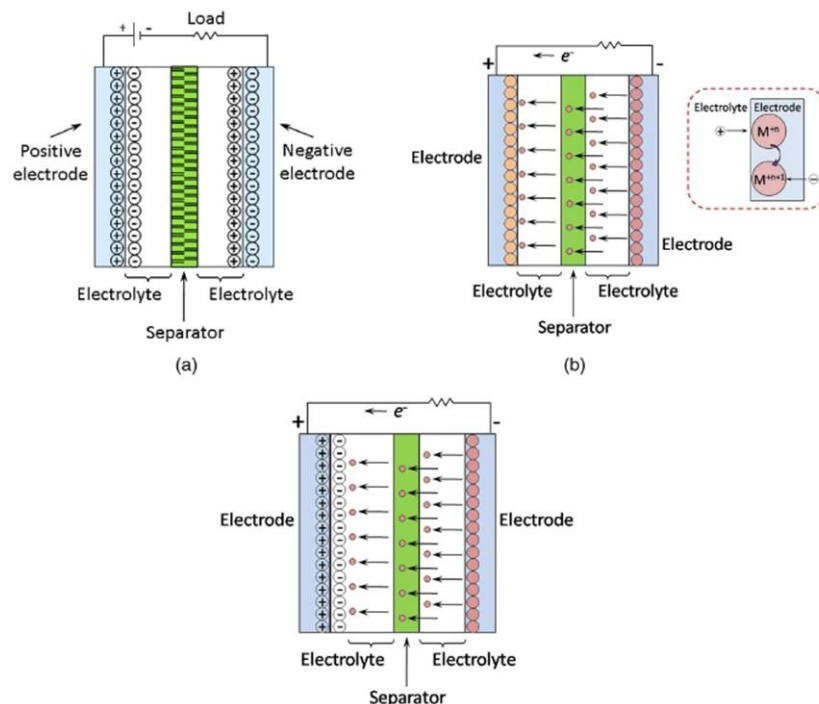


Figure 2-3 Schematic representation of three types of Supercapacitor: (a) EDLC; (b) Pseudocapacitor; (c) Hybrid Capacitor. Copyright 2018 by American Society of Civil Engineers.

### **2.5.1 Composite Hybrid**

Composite electrodes combine carbon-based materials with either conducting polymer or metal oxides in a single electrode, due to this we can say that a single electrode will have both physical as well as chemical charge storage mechanisms. Carbon based materials have capacitive double-layer of charge and high specific surface area due to which the contact between pseudocapacitive materials and electrolyte increases. Due to Faradic reaction, pseudocapacitive material increases capacitance in composite hybrid electrode [48].

There are two different types of composites hybrid capacitor:

1. Binary composites
2. Ternary composites.

In binary composites, two different electrode materials are involved, while in ternary composites three different electrode materials are used to form single electrode.

### **2.5.2 Asymmetric Hybrid**

In asymmetric hybrids Non-faradic and Faradic processes are combined by coupling and EDLC with a Pseudo capacitor electrode. They are set in this way that for negative electrode carbon material is used while for positive electrode either metal oxide or conducting polymers are used [48].

### **2.5.3 Battery Type Hybrid**

In battery type hybrid, two different electrodes are combined same as asymmetric hybrids, but in this case, they are made by combining a battery electrode with supercapacitor electrode. This type of capacitor is formed to use the properties of both supercapacitors and batteries [48].

## **2.6 Electrode Materials**

The parameters that depends on the type of electrode materials used in supercapacitors are charge storage and capacitance.

### 2.6.1 Carbon Materials

For the fabrication of supercapacitor carbon and different types of carbon materials are mostly used. There are following reasons due to which we use carbon and its various types:

1. High surface area
2. Low cost
3. Availability
4. It has established electrode production technologies

The charge storage mechanism used by carbon type materials is electrochemical double layer which is between the electrode and electrolyte. Due to this the capacitance mostly relies on the surface area available to electrolyte ions. The important factors that effects the electrochemical performance are [55-57]:

1. Specific surface area
2. Pore shape and structure
3. Pore size distribution
4. Surface functionality
5. Electrical conductivity

The carbon materials used as electrode materials are:

- ❖ Activated carbon
- ❖ Carbon aerogels
- ❖ Carbon nanotubes
- ❖ Graphene

#### 2.6.1.1 Activated Carbon

The most commonly used electrode material is activated carbon (AC) because it have large surface area, good electrical properties and reasonable cost [58]. AC can be produced by the activation of different types of carbon materials either by physical or chemical means (e.g. wood, coal nutshell etc.). In physical activation process the treatment of carbon precursors at a high temperature (700-1200°C) in the presence of oxidizing gases like air, CO<sub>2</sub> and steam is involved. In chemical activation case ,it is carried out at a lower

temperature (400-700°C) using activating agents such as phosphoric acid, sodium hydroxide, potassium hydroxide, and zinc chloride [39].

#### *2.6.1.2 Carbon Nanotube*

After the discovery of CNT very significant development take place in the field of science and technology of carbon materials. In a supercapacitor the resistance of the components is the main factor which tell about the power density. CNT get great attention as an electrode material for the application of supercapacitor due to its unique properties like porous structure, good thermal, mechanical and electrical properties [59-61]. CNTs are produced by catalytic decomposition of hydrocarbons and by carefully using different parameters, it becomes possible to produce nano structures in different conformations and in controlled crystalline structure. CNT unlike other different carbon-based electrodes, have mesopores that are interconnected. This property gives a continuous charge distribution which uses all the reachable surface area.

#### *2.6.1.3 Graphene*

Recently graphene has been significant attention in research as well as in industrial area. Graphene is a 2D layer structure of unique carbon material which has great potential for energy storage device applications like supercapacitor because of its unique characteristics of very high electrical conductivity, large surface area and chemical stability [62, 63]. Recently, graphene is most extensively used in supercapacitor application because when graphene is used as electrode material of supercapacitor it does not depend on the pores distribution at solid state, unlike other carbon materials such as ACs and CNTs etc. [64, 65].

### **2.6.2 Metal Oxide**

Metal oxides are other alternative materials used in electrodes fabrication materials for supercapacitor application because they have high specific capacitance and low resistance, which makes it easier to form supercapacitors with high energy and power. The commonly used metal oxides for supercapacitor application are following [66-68]:

1. Nickel oxide (NiO),
2. Ruthenium dioxide (RuO<sub>2</sub>),

3. Manganese oxide ( $\text{MnO}_2$ ),
4. Iridium oxide ( $\text{IrO}_2$ ).

Metal oxides production cost is lower, and it uses milder electrolyte which make them a suitable alternative.

### **2.6.3 Conducting Polymers**

Conducting polymers have been extensively use as electrode material for supercapacitor application because they can be easily produce and have low cost [69]. Conducting polymers have a high capacitance and conductivity value as compare to other electrodes that are formed of carbon. The conducting polymers can be used in different electrode configurations such as, the n/p type configuration, in this configuration n doped is negatively charged and p doped is positively charged electrodes are used which gives a high energy and densities [48].

### **2.6.4 Composites**

Hybrid type supercapacitors mostly used composite materials. Composite materials contain combinations of different carbon materials with either conducting polymers or metal oxides, therefore they have properties of both EDLC and pseudo capacitor materials. Electrodes for supercapacitor made of CNT and polypyrrole mixtures exhibit higher capacitance value to electrodes that are either totally based on CNTs or polypyrroles [70, 71].

## **2.7 Fabrication Methods**

There are many different methods of material synthesis of supercapacitor. Those synthesis methods are electrochemical deposition, chemical vapor deposition (CVD), chemical bath deposition and the sol-gel method. Also, there are numerous methods of electrodes fabrication for supercapacitor, including spray coating, inkjet printing, and direct writing which include laser scribing technique.

### **2.7.1 Electrode Fabrication Methods**

For supercapacitor application the fabrication of electrodes can be done by using printing techniques. The Printing techniques include inkjet printing, casting and spray painting in which printing can be done directly on surface or by using any template. The main

advantage of printing technique is that larger area surfaces can be easily coated. Other advantage of printing technique is that it can easily deposit coating material on uneven or unusual surfaces such as on flexible polymer sheets or fabric and paper. Printable material solution is sprayed on a substrate surface. The example of solution of printable material is CNTs in a solvent. This printed film of CNTs work as an electrode in supercapacitor.

The spray technique has been used to make CNTs based electrodes on plastic substrates, these also work as charge collectors[72]. Inkjet printing technique is used to make very thin electrodes using carbon nanotubes as an ink material on fabrics and flexible substrates. This is very easily method of fabricating thin electrodes. Another printing method is direct writing method in which for fabricating a supercapacitor graphite rod is used on cellulose paper[73]. The advantage of this method is that it does not required any solvent and can find specific applications. The electrode fabrication procedures in terms of material, advantages and their disadvantages are shown in the **Table 6**. One of the latest electrode fabrication technique is Laser Scribing which we use in our research work for the fabrication of electrode is discuss below.

*Table 6 Different electrode fabrication methods in terms of materials, advantages, and disadvantages. Copyrights 2018 By ASCE*

Synthesis Methods	Materials	Advantages	Disadvantages
Electrochemical deposition method	<ul style="list-style-type: none"> <li>• Metal oxides</li> <li>• Conducting polymers</li> <li>• Ruthenium</li> </ul>	<ul style="list-style-type: none"> <li>• Mass production</li> <li>• Low costs</li> <li>• Precise control on uniformity and film thickness</li> </ul>	<ul style="list-style-type: none"> <li>• Process set up</li> <li>• Current or voltage required</li> </ul>
CBD	<ul style="list-style-type: none"> <li>• PANI</li> <li>• Ruthenium oxide</li> </ul>	<ul style="list-style-type: none"> <li>• Simplicity</li> <li>• Low temperature</li> <li>• Inexpensive</li> <li>• Large-area substrates</li> </ul>	<ul style="list-style-type: none"> <li>• Limited flexibility</li> <li>• Low material yield</li> </ul>

<b>CVD</b>	<ul style="list-style-type: none"> <li>Carbon materials (CNTs, nanofibers, and graphene)</li> </ul>	<ul style="list-style-type: none"> <li>High material yield than CBD</li> <li>Good film uniformity</li> </ul>	<ul style="list-style-type: none"> <li>Expensive equipment and relatively high costs</li> </ul>
<b>Sol-gel</b>	<ul style="list-style-type: none"> <li>Carbon aerogels</li> <li>Carbon-ruthenium</li> <li>SnO<sub>2</sub>, MnO<sub>2</sub></li> </ul>	<ul style="list-style-type: none"> <li>Low costs</li> <li>Controllable film texture</li> <li>Composition</li> <li>homogeneity</li> <li>Structural properties</li> </ul>	<ul style="list-style-type: none"> <li>Complicated process</li> </ul>
<b>Chemical precipitation</b>	<ul style="list-style-type: none"> <li>Nickel oxide/carbon</li> <li>MnO<sub>2</sub>/nanofibers</li> <li>MnO<sub>2</sub>/CNTs</li> </ul>	<ul style="list-style-type: none"> <li>Allows synthesis of composite electrode materials</li> <li>Efficient</li> <li>Easily implemented</li> </ul>	<ul style="list-style-type: none"> <li>May generate a waste product</li> </ul>

## 2.8 Laser Scribing Technology

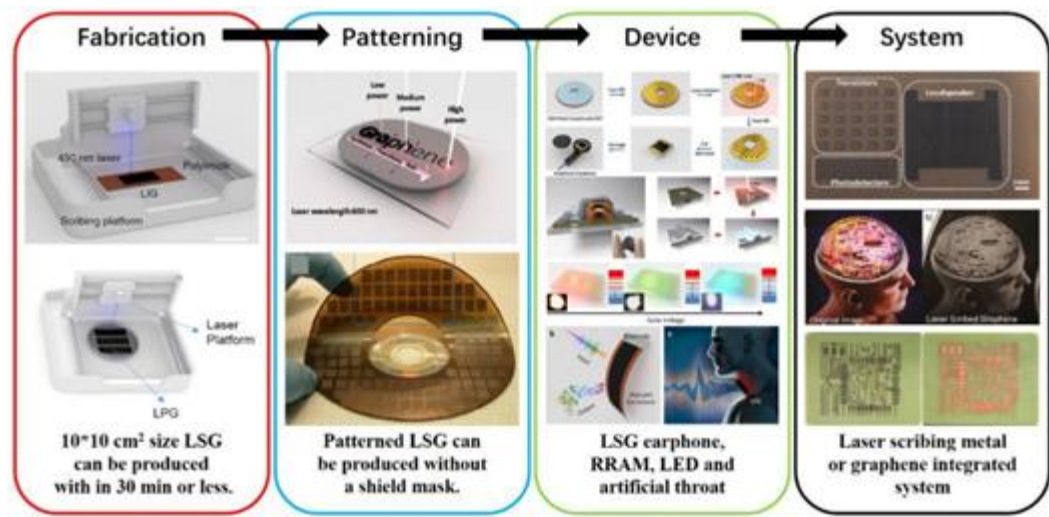


Figure 2-4 Illustrates the four different steps of Laser scribing i) fabrication ii) patterning iii) device iv) System. Copyright 2018 by the Japan Society of Applied Physics.



Laser scribing technology consists of four main processes as shown in the Figure 2.4. During the fabrication process materials which can be photo reducible are used such as GO, polyimide, polyetherimide and polyethersulfone[74]. In the next step, substrates are patterned by a certain laser depending on the type of substrate materials used. The most commonly used material which is reduced by laser or in other words scribed by laser is graphene oxide (GO) and polyimide (PI). Laser scribe the surface of GO into rGO and PI into rPI making conductive tracks. Different types of lasers have been for this purpose such as femtosecond-laser, Zhang et al.[75] used this laser to do laser scribing for the first time. Other lasers have been used for laser scribing are nanosecond laser, Nd:YAG, Nd:YVO4, KrF, CO2, diode, fiber laser and DVD burners. These all have been used to form graphene.

Table 7 Common substrate materials and application of LSG devices. Copyright 2018 by The Japan Society of Applied Physics.

Substrate	Laser parameter	Carbon source	Resistance	Application
PET/DVD disc	DVD burner	GO	1738 S/m	Supercapacitor
			8.2 k $\Omega$	Earphone
			2.3 k $\Omega$	Transistor
			2.3 k $\Omega$	Loudspeaker
			2.3 k $\Omega$	Photodetector
			—	RRAM
			2.3 k $\Omega$	Press sensor
			165 $\Omega/\mu\text{m}$	LED
PI,silicon wafer,plastic dish, glass lens,PET, cloth,leaf	650 nm	GO	158.7 $\Omega$	Heater
PI,PEI	CO <sub>2</sub> IR laser	PI, PEI	25 S/cm	Supercapacitor
SPEEK	—	SPEEK	—	Supercapacitor
PDMS	CO <sub>2</sub> IR laser	PI	60 $\Omega/\square$	Strain sensor
PI	450 nm	PI	—	Intelligent throat

Glass, sticky note,PI, spectacle lens,a butterfly wing	650 nm	GO	763 $\Omega$	Photodetector
---	--------	----	--------------	---------------

Basically, the substrate reduction process takes place as the oxygenated functional groups ( $\text{OH}^{-1}$ ) are converted into oxygen ( $\text{O}_2$ ). The gases are evolved, leaving behind rGO or rPI, making the distance between the layers of graphene larger and a porous structure is formed.

### 2.8.1 Laser Scribing Based on Graphene Oxide

GO has different oxygenated functional groups such as C=O, OH- and COOH present in its structure, when these groups are removed graphene can be formed. Tian et al.[76] made electroacoustic and optoelectronic devices by laser scribing of GO. Polymer film of PET was attached on a DVD disc burner. This DVD disc was then coated with GO dispersion. The laser scribing process was done through DVD burner, initially GO film resistance was around 580 M $\Omega$ , however, after laser scribing the resistance were around 2-8 k $\Omega$ . Deng et al. [77]drop-casted GO on different substrates including butterfly wing, leaves, glasses, polyimide etc. and did laser scribing. They found three different regions of scribing depending on the power of the laser

➤ **Growth region**

In this region, the laser power is around 1-60mW and GO is converted into rGO (growth) but the carbon species remains the same having loosely packed layers. Hence the thickness increases in growth region due to the gasification of hydrogen and oxygen.

➤ **Transition region**

In this region, the laser power between 70-180mW, the growth takes place but at the same time etching also takes place at higher laser intensity. As the LSG is generated by the laser it is being etched at the same time. The thickness in this region remain the same as of GO.

➤ **Etching region**

In this region, the laser power is higher than 190mW, no growth takes place in this region and only etching takes place. Due to this all the GO film is etched and leaves behind the substrate.

### **2.8.2 Laser Scribing Based on Polymers**

Graphene or reduced graphene can be produced by various polymers, as discovered by Lin et al.[78] converted PI films into reduced graphene via one-step processing technique which is laser scribing. LSG was also produced by polyetherimide (PEI). However, LSG cannot be produced by irradiating PVA, PMMA, PET and other polymers. Dorin et al.[79]developed a conductor insulator composite using DuPont<sup>®</sup> polyimide sheets. The resistivity of the finished product was  $6 \Omega\text{cm}^{-1}$ . Lamberti et al. [80]reported a method of scribing a polymer sulfonated poly (ether ether) ketone (SPEEK). Just like PI this is a one-step process.

## **2.9 Aims and Objectives**

1. Fabrication of a supercapacitor which have high storage energy and is fabricated on a flexible substrate.
2. Device fabrication having low cost
3. The supercapacitor must be durable, so it can it perform well under hundreds of charge/discharge cycles.
4. The supercapacitor should have repeatability, the percentage capacitance should not change under hundreds of cycles.
5. Supercapacitor having fast charge/discharge time.
6. Easily commercialize able.

## Chapter 3: Methodology

In this research work, a supercapacitor is fabricated which is very cost-effective, easily developed, having high storage energy, fast charge and discharge cycles and highly flexible. In this research polyimide is selected as substrate material and the laser scribing technology was adopted for fabrication.

### 3.1 Materials Required

All materials used for this research work were purchased from different sources and are mentioned as follows:

- ❖ Polyimide (PI) sheet having thickness of 0.25mm (Chinese Supplier)
- ❖ Poly (vinyl Alcohol) PVA (Sigma)
- ❖ Silver Conductive paste (Agar Technologies UK)
- ❖ Copper Tape (Chinese Supplier)
- ❖ Kapton Tape (DuPont USA)
- ❖ Sulfuric Acid (Sigma)
- ❖ Phosphoric Acid (Sigma)
- ❖ Potassium Hydroxide (Sigma)
- ❖ Potassium Iodide (Sigma)
- ❖ Deionized (DI) Water (Thermal transport lab)

#### 3.1.1 Polyimide Substrate

In this work we used 200um polyimide sheet for substrate material. Polyimide have been used in many different fields of electronics it is made as thermoset polymer. Due to its practical and promising application, it is commonly available in market. Polyimide films with different molecular structure used in different applications according to their performance. Equimolar aromatic diamine and Tetracarboxylic dianhydride are reacted together in N,N0-dimethylacetamide (DMAc) to form Aromatic polyamides. The process is carried out by dehydrating the product of poly (amic acid) by conducting a chemical

method which is known as imidization. For instance, a polyimide “PMDA/ODA” is characterized by its parents pyromellitic dianhydride (PMDA) and 4,4'-oxydianiline (ODA). Some of the polyimides are commercially available like Kapton which is often used in literatures. Former part of repeating unit of a polyimide is known as “imide part” and the latter part is “bridging part”. Most of the literatures in which Kapton is used have the repeating unit PMDA/ODA. Commercially available film is Kapton which is described above and the polyimide which is synthesized in a laboratory is called PMDA/ODA[81].

### 3.1.2 Poly (Vinyl Alcohol) PVA

Poly (vinyl alcohol) having molecular weight 70,000 was used. PVA was first introduced to industrial application is early 1930s. It is one of the very first water soluble polymers, one of a very few synthetic biodegradable polymers and has good physical properties[82]. Polyvinyl Alcohol (PVA) is obtained by the polymerization of vinyl alcohol. It is a synthetic polymer and can be prepared by replacing the acetate groups with hydroxyl groups in polyvinyl acetates. It has several uses in commercial and industrial applications like manufacturing of paper, textiles and printing. Also, in pharmaceutical uses like in the

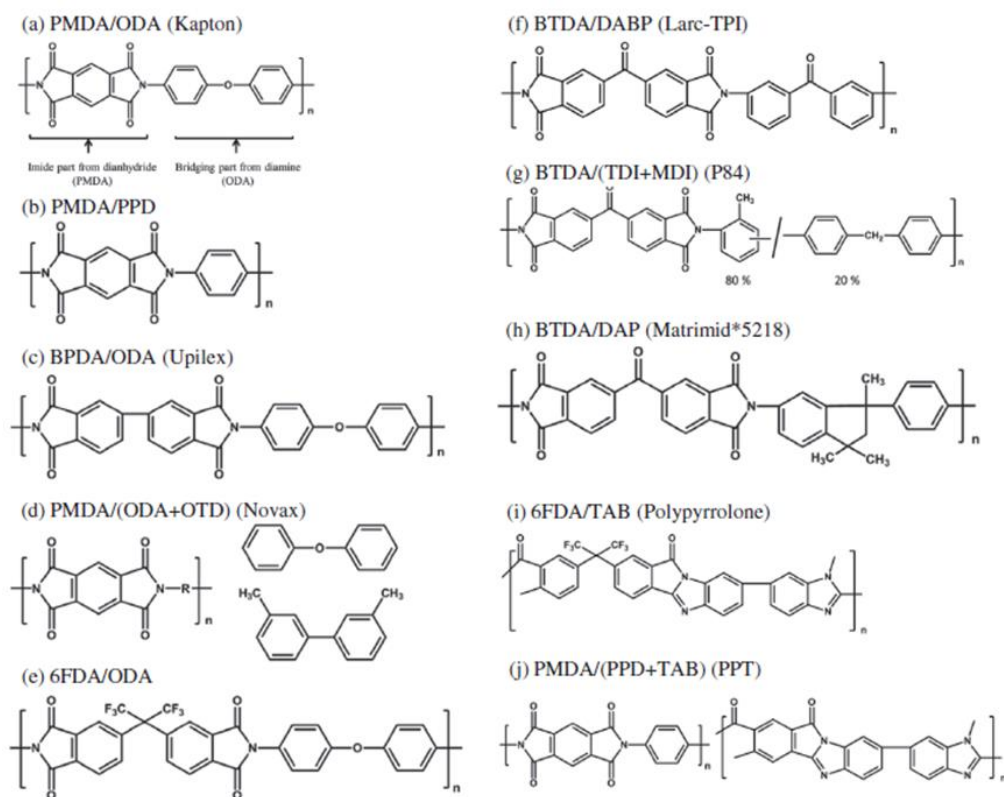


Figure 3-1 Different repeating units of polyimide, Copyright 2018 by The Elsevier Ltd.

making of ophthalmic lubricant for prevention of dry eyes. It is also used in surface coatings, artificial sponges and many other products.

With the process of adding suitable impurities, polyvinyl alcohol (PVA) can be distinctly influenced. PVA is a good insulating material having low charge storage capability and conductivity[83]. PVA is highly reactive in nature because of its secondary alcohol functionality. Such solubility feature gives it a significant importance in environmental and green chemistry applications [84]. PVA has found its way in greater industrial use because of its chemical properties. However physical properties of PVA may vary according to its preparation unlike other polymers. PVA properties can be changed by the polymerization conditions as well as by the hydrolysis conditions[85].

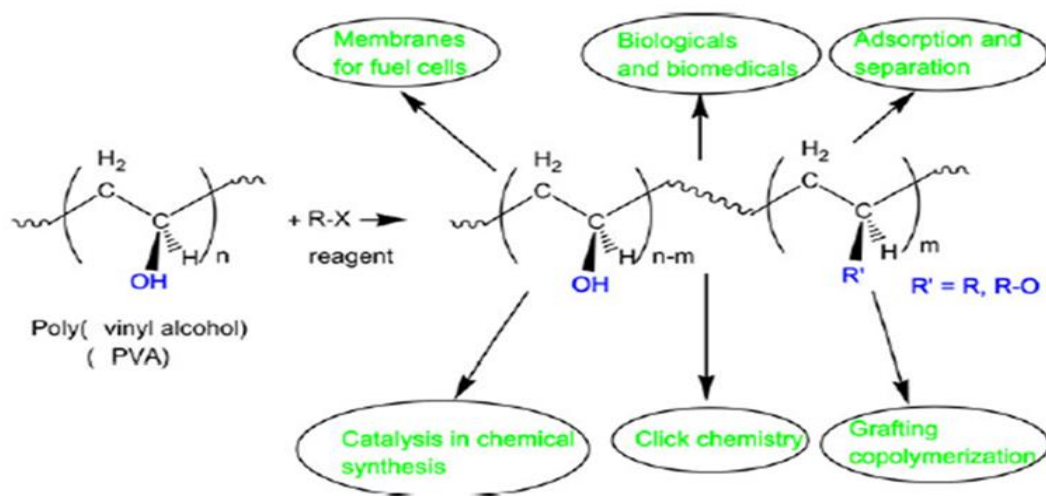


Figure 3-2 Functionalization of Poly (vinyl Alcohol), Copyright 2018 by Taylor & Francis Group, LLC.

### 3.2 Apparatus for Electrolyte Preparation

In this research work, we prepare different types of liquid as well as gel electrolytes for our supercapacitor application. For making different types of gel electrolyte, Poly (vinyl alcohol) with different acids or base were mixed.

For the preparation of electrolyte, the following apparatus was used:

- ❖ Beakers
- ❖ Aluminum Foil
- ❖ Stirrers

- ❖ Heating Plate
- ❖ Spatula

### **3.3 Instrumentation**

Instrumentation required for supercapacitor fabrication, patterning, material characterization and device characterization and measurement is as follows:

- ❖ OSRAM Diode Laser Scriber ( $\lambda=450\text{nm}$  near UV)
- ❖ STOE  $\theta$ - $\theta$  XRD diffractometer
- ❖ JEOL Analytical SEM (JSM- 6490A)
- ❖ FTIR
- ❖ Raman Spectroscopy
- ❖ Biologic EC-LAB (VSP)
- ❖ Two Probe Station
- ❖ Digital Multimeter (DMM)

#### **3.3.1 Laser Engraver**

A laser engraver of 450nm wavelength having maximum power of 500mW was used to reduce the polyimide surface and convert it into a carbonized structure[86]. Figure 3.3(a) shows a photograph of the laser setup. It is a 2D laser engraver setup in which stepper motors are used to move the laser in the X-Y direction. Laser engraver have a software which have many features like writing, import images, rotate or reverse your image, intensity levels and carving time. Figure 3.3 (b) shows the photograph of software in which we import the image in it. This laser instrument dose not required any mask for the fabrication and any design can be drawn by importing the image into it. For making desired image we can used any software like MS paint or AutoCAD. Then we import that image into the controlled laser software and click on start button to turn laser on.

By changing the laser intensity different types of supercapacitors were formed having different characteristics. The laser intensity and carving time can be varied by using simple user friendly laser software. Supercapacitor of required design can also be formed very easily by importing the image into the software.

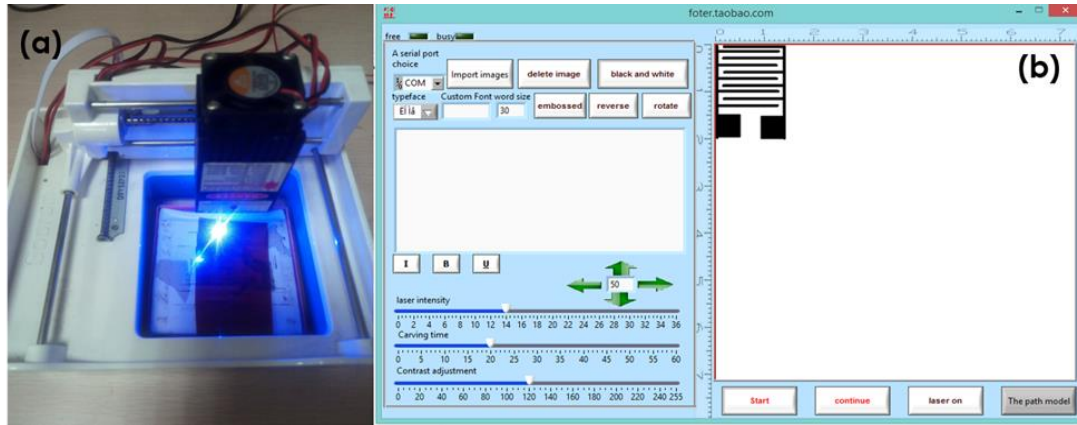


Figure 3-3 (a) Photograph of laser engraver setup, (b) Software used for laser engraver

### 3.3.2 Two Probe Station

In this research work we used two probe station for the measurement of conductivity of electrodes formed by laser. It is a very sensitive setup which measure change in resistance very accurately. Two probes attached on the corners of the reduced polyimide surface, the current verse voltage graph of respective surface formed on the computer.

A probe station has container which is placed in vacuum chamber. To test the semiconductor device, we attached it into the container of the liquid. For testing device electrical contacts required. A microscope is attached with the vacuum externally to see the placement of the contact wires on the devices which is tested. One side of the vacuum chamber is formed of plastic material this is used to see from microscope. These electrical devices which are tested required proper connection of test equipment to the electrical contact wires. Due to this proper connection of equipment with contact wires gives reliable and effective results of the devices under the same temperature and pressure at which a device can perfectly operate.



### 3.3.3 Digital Multimeter (DMM)

For testing the resistance of the polyimide before and after the laser irradiation a digital multimeter (DMM) was used. By using the DMM a change in resistance of the polyimide was easily detected. Polyimide (PI) is a nonconductive material having very high resistance and after laser irradiation we can see that the DMM show resistance of few ohms.

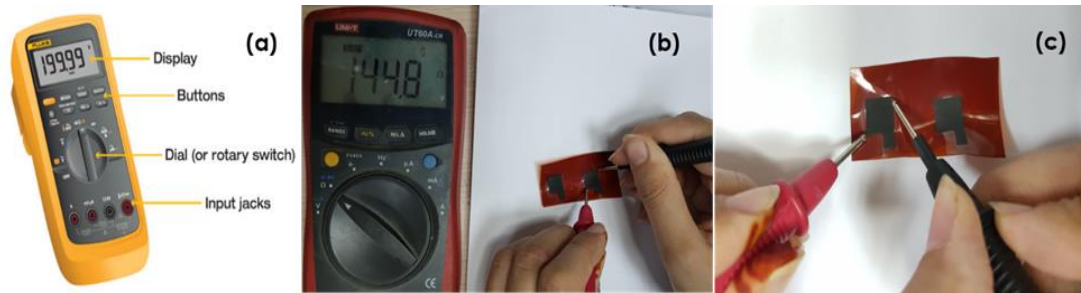


Figure 3-4 (a) Photograph of Digital multimeter (DMM) (b) Resistance measurement of electrodes using DMM, (c) Zoomed image of electrodes

A **digital multimeter (DMM)** is a test tool which is used to measure the electrical values like voltage, current, resistance and capacitance. By this we can also check the electrical connectivity of devices. This is a standard tool which is used in electrical and electronics industries. DMM has the ability to do measurements with greater accuracy due to which it replaced needle-based analog meters. The first DMM was introduced by Fluke in 1977. The DMM have the combined testing capability like the voltmeter we can measure voltage in volts, ammeter for finding current in amperes and Ohmmeter for measuring resistance in Ohms. In advanced DMM more features are also present like we can check capacitance and inductance of devices.

### 3.4 Electrodes Formation

For supercapacitor fabrication the main step is electrodes preparation. For making flexible supercapacitor we used polyimide as our substrate material. Polyimide is an insulating material, it is non-conductive in nature. For energy storage electrode material should be porous due to which energy can be stored in the pores. In laser technology for making supercapacitor we need to design it first, which type of supercapacitor we want to fabricate. Here we made stacked supercapacitor, which is in the form of square box. For making a single supercapacitor device two electrodes were required.

In stack type supercapacitor, an area of  $1\text{cm} \times 1\text{cm}$  of polyimide was reduced by laser which converts polyimide surface into the carbonized material having porous structure. An additional elongated area, measuring  $0.2\text{cm} \times 1\text{cm}$  was reduced besides the  $1\text{cm} \times 1\text{cm}$  square which act as an electrode to connect to external measurement apparatus. By changing the laser intensity different types of supercapacitors formed having different characteristics.



Figure 3-5 Image of two stack type supercapacitor electrodes

### 3.5 Electrolyte Preparation

The electrolyte plays a very important role in supercapacitor energy storage. Supercapacitor energy storage depends on electrolyte nature which includes following points

1. The size and type of ion
2. The ion concentration and amount of solvent
3. The interaction between the ion and solvent
4. The interaction between electrode and electrolyte material
5. Potential window of electrolyte

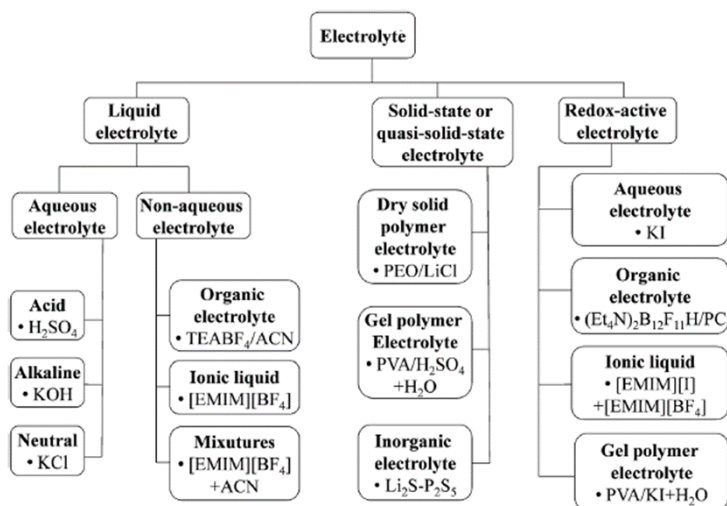


Figure 3-6 Classification of electrolyte for supercapacitor, Copyright 2018 by the Royal Society of Chemistry.

Electrolytes are of different types as shown in **Figure 3-6** and ions having different conductivity is shown in **Figure 3-7**

Ion	Bare ion size (Å)	Hydrated ion size (Å)	Ionic conductivity (S cm <sup>2</sup> mol <sup>-1</sup> )
H <sup>+</sup>	1.15 <sup>b</sup>	2.80 <sup>b</sup>	350.1 <sup>a</sup>
Li <sup>+</sup>	0.60 <sup>c</sup>	3.82 <sup>b,c</sup>	38.69 <sup>a</sup>
Na <sup>+</sup>	0.95 <sup>c</sup>	3.58 <sup>b,c</sup>	50.11 <sup>a</sup>
K <sup>+</sup>	1.33 <sup>c</sup>	3.31 <sup>b,c</sup>	73.5 <sup>a</sup>
NH <sub>4</sub> <sup>+</sup>	1.48 <sup>b,c</sup>	3.31 <sup>b,c</sup>	73.7 <sup>a</sup>
Mg <sup>2+</sup>	0.72 <sup>a,b</sup>	4.28 <sup>b,c</sup>	106.12 <sup>a</sup>
Ca <sup>2+</sup>	1.00 <sup>b</sup>	4.12 <sup>b,c</sup>	119 <sup>a</sup>
Ba <sup>2+</sup>	1.35 <sup>c</sup>	4.04 <sup>c</sup>	127.8 <sup>a</sup>
Cl <sup>-</sup>	1.81 <sup>a,c</sup>	3.32 <sup>b,c</sup>	76.31 <sup>a</sup>
NO <sub>3</sub> <sup>-</sup>	2.64 <sup>c</sup>	3.35 <sup>c</sup>	71.42 <sup>a</sup>
SO <sub>4</sub> <sup>2-</sup>	2.90 <sup>c</sup>	3.79 <sup>c</sup>	160.0 <sup>a</sup>
OH <sup>-</sup>	1.76 <sup>c</sup>	3.00 <sup>b,c</sup>	198 <sup>a</sup>
ClO <sub>4</sub> <sup>-</sup>	2.92 <sup>c</sup>	3.38 <sup>c</sup>	67.3 <sup>a</sup>
PO <sub>4</sub> <sup>3-</sup>	2.23 <sup>d</sup>	3.39 <sup>d</sup>	207 <sup>a</sup>
CO <sub>3</sub> <sup>2-</sup>	2.66 <sup>c</sup>	3.94 <sup>c</sup>	138.6 <sup>a</sup>

Figure 3-7 shows the sizes of bare ions, hydrated ions, and ionic conductivity values. Copyrights by 2018 The Royal Society of Chemistry.

For checking our device performance, we make few different types of electrolytes. Electrolytes that we used can be divided into two main categories

1. Liquid or Aqueous electrolytes
2. Gel Electrolytes

### 3.5.1 Liquid or Aqueous Electrolytes

Liquid or Aqueous electrolytes were formed by mixing 1g or 1ml of Acid or base in 10ml or deionized water. The electrolyte that used in this research work is potassium hydroxide and phosphoric acid with water. The maximum capacitance value achieved by liquid potassium hydroxide electrolyte is 2.02uF/cm<sup>2</sup> and by liquid phosphoric acid is 2.24uF/cm<sup>2</sup>.

### 3.5.2 Gel Electrolytes

Hydrogel electrolytes used for supercapacitor application which have been already studied include potassium poly (acrylate) (PAAK), polyvinyl alcohol (PVA), poly (acrylamide) (PAAM), and polyvinyl alcohol/poly(acrylic acid) (PVA/PAA). Among all these polymers, PVA is a more attractive polymer hydrogel electrolyte because it has the following properties[87].

1. Biodegradable

2. Nontoxic
3. Inexpensive
4. Chemically stable
5. High structural integrity and good mechanical properties
6. High Ionic conductivity

Six different gel electrolytes are mostly used for the supercapacitor application which includes ( $\text{H}_3\text{PO}_4$ ,  $\text{H}_2\text{SO}_4$ , KOH, NaOH, KCl, NaCl). These electrolytes are formed by mixing 0.01 mol acid or base and 1 g of PVA in 10 mL deionized water by doing stirring and heating at specific temperature[52]. The polymer gel electrolyte that we used in this work is phosphoric acid with PVA and potassium hydroxide and potassium iodide with PVA. The method for the preparation of both electrolytes is almost identical. By using this method we can prepare any type of acidic or base gel electrolyte.

#### *3.5.2.1 Phosphoric Acid with PVA*

The polymeric gel electrolyte PVA/ $\text{H}_3\text{PO}_4$  was made by mixing and stirring 10ml of DI water, 1ml of  $\text{H}_3\text{PO}_4$  and 1g PVA and heated at 80°C overnight [86, 88]. As a result, a gel type electrolyte is formed, which is coated on reduced polyimide and then placed in an oven at 50°C for 15 minutes to remove the excess water present in the electrolyte.

#### *3.5.2.2 Potassium Hydroxide with PVA*

The PVA and KOH polymer gel electrolyte can be prepared by a solution-casting method. In this method, 1 g of PVA and 1 g KOH is dissolved in 10ml of deionized water with continuous stirring at 80 C for 4 h. when this solution is completely dissolved it looks homogeneous in appearance. The excess water present in the electrolyte was evaporated by placing it in a vacuum oven at 80 C. After this we get PVA–KOH hydrogel electrolyte[89].

### 3.5.2.3 Potassium Hydroxide and Potassium Iodide with PVA

PVA–KOH–KI gel electrolyte was prepared by dissolving 1g PVA, 1g KOH and 1g KI in 10ml deionized water at 80C for few hours. A homogenous clear solution is formed and after this, more stirring was done for 2-3 hour to remove excess water and get gel electrolyte [90].

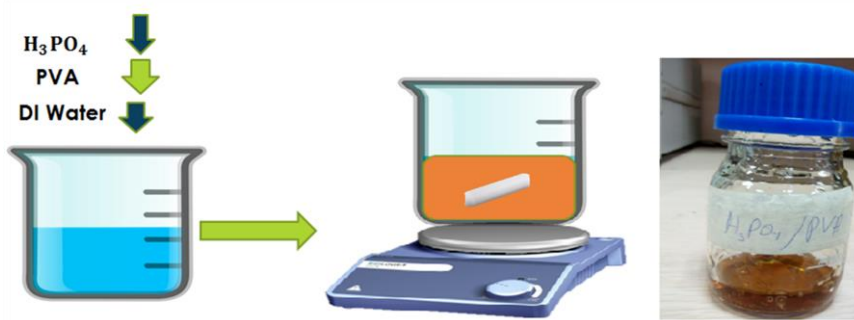


Figure 3-8 Phosphoric acid with PVA gel electrolyte synthesis

## 3.6 Device Formation

For supercapacitor device fabrication electrodes assembly and proper electrolyte deposition is necessary. Electrode and electrolyte preparation method is discussed above. Here we make different type of stacked supercapacitors by changing laser intensity and by changing electrolyte. Supercapacitor properties can be varied by changing the reduced area of electrode. There are many different kinds of supercapacitors available, we made stacked supercapacitor for it is not easy to fabricate but its area can also be customized according to the requirements.

For stacked supercapacitor, an area of 1cm × 1cm of polyimide was reduced by laser which converts it into a carbonized structure with porous conductive surface. Hence, two electrodes of 1cm × 1cm were made using same laser intensity followed by uniform electrolyte deposition. The electrodes were then placed in the lab oven for 15mint at 50° Celsius for removal of excess water. The electrodes were then place together ensuring no

air space or direct contact between two electrodes for it can cause ill-functioning of the device e.g, leakage current in the later case.

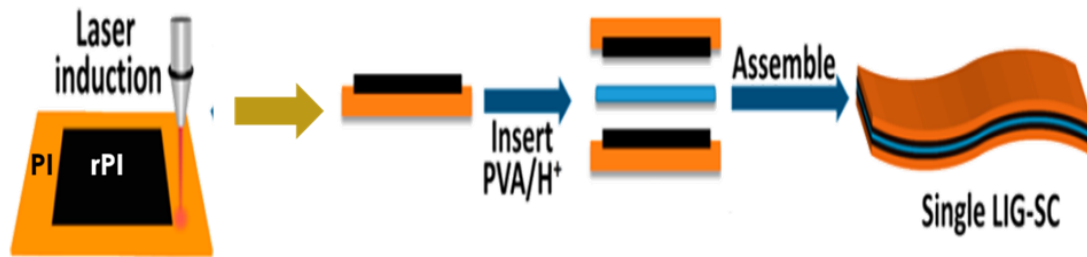


*Figure 3-9 Schematic diagram of stacked supercapacitor*

### **3.7 Device Packaging**

For device packaging lamination machine was used. Supercapacitor was coated into the lamination sheet and then passed this into the lamination machine. As polyimide has a very high melting point, therefore passing it into the hot rod does not affect its properties.

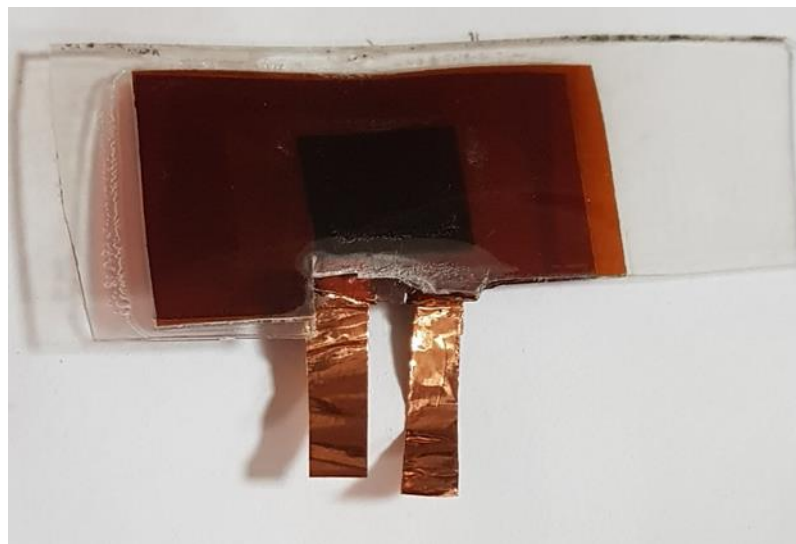


*Figure 3-10 Packed form of stacked supercapacitor*

## Chapter 4: Characterization Techniques

### 4.1 Fourier Transform Infrared Spectrophotometer

FTIR spectrophotometric analysis involves the interaction of infrared radiations with matter. The energy of infrared radiations is low therefore when they interact with matter only vibrational and rotational movement is observed. The infrared region present in electromagnetic spectrum is separated into three portions i.e.

- Near Infrared region
- Far infrared region
- Mid infrared region

Infrared spectroscopy is also called as functional group spectroscopy. It is used for the functional group analysis of a chemical compound and from mode of transition and absorption value one can identify the chemical nature of given compound in the simple. Those chemical substances are identified in FTIR analysis in which a change in dipole moment occur when infrared radiations fall on them. The change in dipole moment is necessary. In diametric symmetric molecules no dipole moment change is observed therefore they do not show any vibrational motion in infrared region for example nitrogen. Asymmetric diatomic molecules like CO give IR spectrum due to change in its dipole moment as a result of interaction with infrared radiations. The complex molecules like organic molecules have many bonds thus can vibrate in different ways. There are basically two types of vibrations phenomena observed in FTIR spectroscopy i.e.

- i. Stretching vibrations
- ii. Bending Vibrations

In stretching vibrations, the bond length changes as a result of interaction of light with matter. There are two types of stretching vibrations i.e. symmetric or asymmetric. Whereas in bending vibration only bond angle changes. Bending vibrations have four types i.e.[91].

- i. Scissoring
- ii. Rocking

iii. Wagging

iv. Twisting

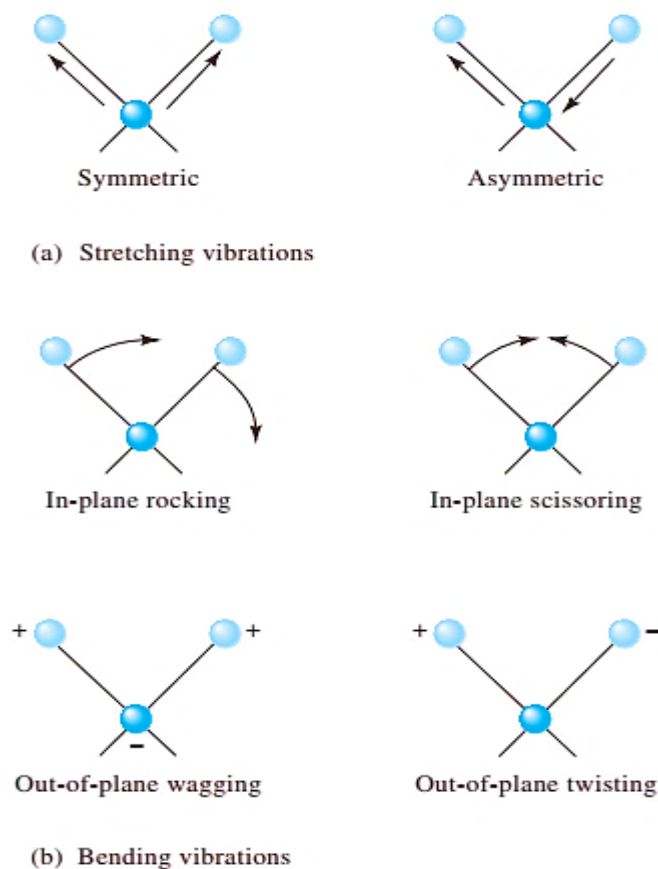


Figure 4-1 Mode of vibrations in FTIR Spectroscopy

#### 4.1.1 Instrumentation

The infrared spectrum of a sample is formed when infrared light passes through the sample. If the frequency of infrared radiation matches the frequency of chemical bond present in the analyte, then molecule show the vibrational or rotational motion. The amount of light absorbed by analyte is measured. This gives information about the nature of chemical bond and possible functional groups present in the sample [3].

The basic components of infrared spectrophotometry are

- i. Source of infrared light
- ii. Interferometer



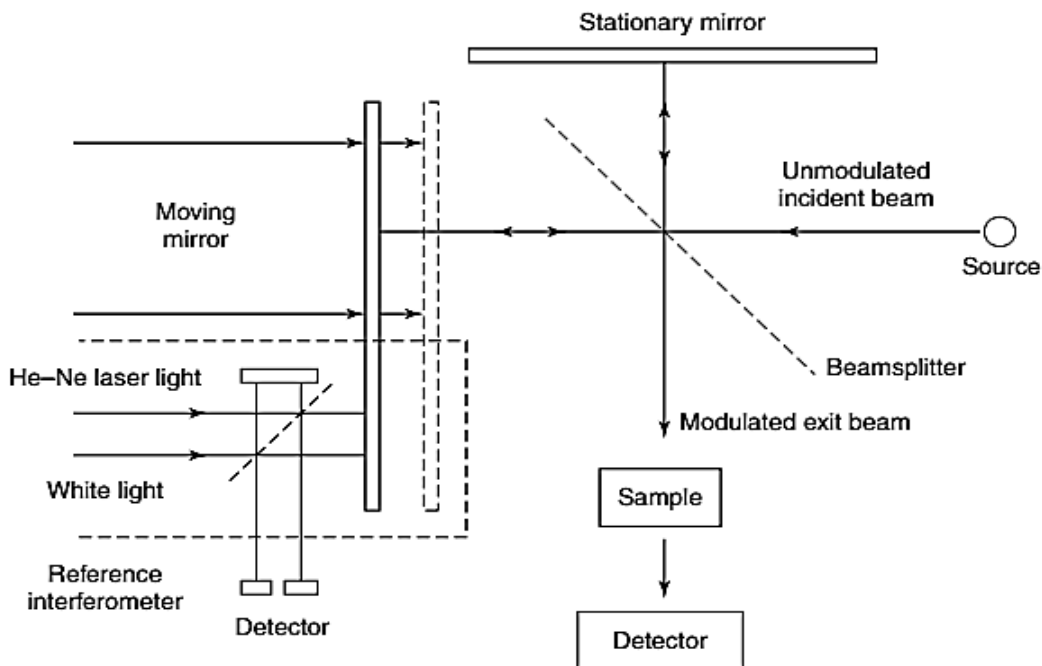


Figure 4-2 Schematic diagram of working of FTIR spectrophotometer [1]

- iii. Sample
- iv. Detector
- v. Amplifier
- vi. Analog to digital converter

## 4.2 Raman Spectroscopy

Raman spectroscopy is a modified form of FTIR technique which is efficient and non-destructive. It is used to know about rotational, vibrational and low frequency modes present in compounds. It provides a fingerprint through which a molecule can be identified. In this technique the monochromatic light is focused on the sample which then interacts with the chemical bonds of the compound. After interaction with the photons of light, molecule shows different vibrational and rotational states. Intensity of Raman scattering is determined by polarizability. The Raman shifts are mainly determined in terms of wave number ( $\text{cm}^{-1}$ ).

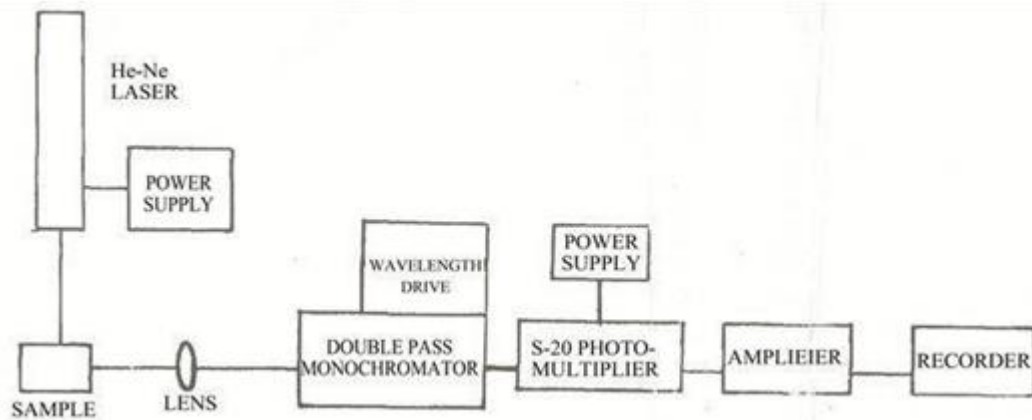


Figure 4-3 Schematic illustration of Raman Spectroscopy

### 4.3 X-ray Diffraction analysis

X-ray diffraction analysis is done to identify structure and degree of crystallinity of the material. It gives information about strains; defects in crystal structure as well as average particle size of crystal can also be calculated by using this. Diffraction analysis is done in this technique. When two wavelengths of same frequency and amplitude pass through a medium in this way the crest and trough superimpose on each other and amplitude of the wave maximizes it leads to formation of constructive interference. But if two waves pass through the sample in such way that crest falls on trough that subtract the influence of each other and resultant destructive interference has minimum amplitude. There are three methods for the analysis of crystal structure i.e.

- Laue Method
- Powder X-ray diffraction
- Rotating crystal structure

Powder x-ray diffraction analysis is most advanced and most commonly used method especially for the characterization of nanomaterials. The crystallite size of nanoparticles in powder x-ray diffraction analysis is done by using two methods i.e.

- Debye Scherrer Method
- Diffractometer Method

The sample used in powder XRD analysis is finally grinded along with Molybdenum or copper as reference materials.

The basic principle of powder X-ray diffraction analysis is that the X-ray fall on the sample and is reflected from the planes of crystal. The interference only occurs at the point where incident angle of beam matches the reflection angle. This phenomenon was described by a scientist Bragg`s and is known as Bragg`s law. The equation of Bragg`s law is;

$$n\lambda = 2d \sin\theta$$

Where,

$n$  = order of interference

$\theta$  = angle of incidence of X-ray beam

$d$  = interlayer distance between planes of the crystal

$\lambda$  = wavelength of incident x-ray beam

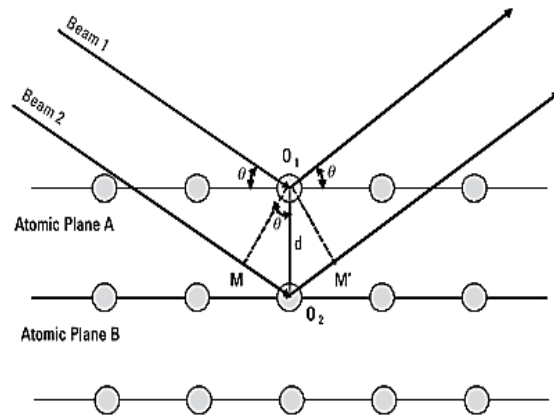


Figure 4-4 X-ray diffraction by planes of crystal [2]

Braggs law states that only that beam of light is reflected by crystal plane where path difference between planes is  $2d\sin\theta$  when all planes are set at an equal distance  $d$  to make constructive interference.

### 4.3.1 Instrumentation

X-ray diffraction machine consists of three basic components i.e.

- i. Source of X-rays or x-ray tube
- ii. Sample holder
- iii. Detector

The X-rays are produced by heating a filament which produces the electrons in cathode ray tube. These electrons are then bombarded on the target material i.e. copper or molybdenum. The targeting electrons have enough energy that they penetrate the crystal structure and excite inner shell electrons. The acceleration and deceleration of these electrons produce waves in X-ray region. These X-rays are then directed on to the sample in sample chamber

When the incident angle of X-rays matches the reflected angle between the planes of crystal constructive interference occurs and it is recorded by the detector.

The data obtained by X-ray diffraction analysis can be used for the measurement of lattice constant of unit cell of crystal, Crystallite size, samples material density and pore fraction. Following are the formulas used for the calculations of all above described values.

For the calculation of Lattice Constant of unit cell of sample material formula is

$$a = \frac{\lambda (h^2 + k^2 + l^2)^{1/2}}{2 \sin \theta}$$

Where,

$\lambda$  = wavelength of X-ray

hkl = miller indices

$\theta$  = is diffraction angle

Formula used for the measurement of crystallite size is Debye Scherrer formula;

$$t = \frac{0.9 \lambda}{\beta \cos \theta}$$

Where,

$\theta$  = diffraction angle

$\lambda$  = Wavelength of X-ray used for analysis

$\beta$  = is full width half maximum (FWHM)

For the calculation of pore fraction of nanomaterials, the formula used is;

$$\text{Porosity Fraction} = 1 - \frac{\rho_m}{\rho_x}$$

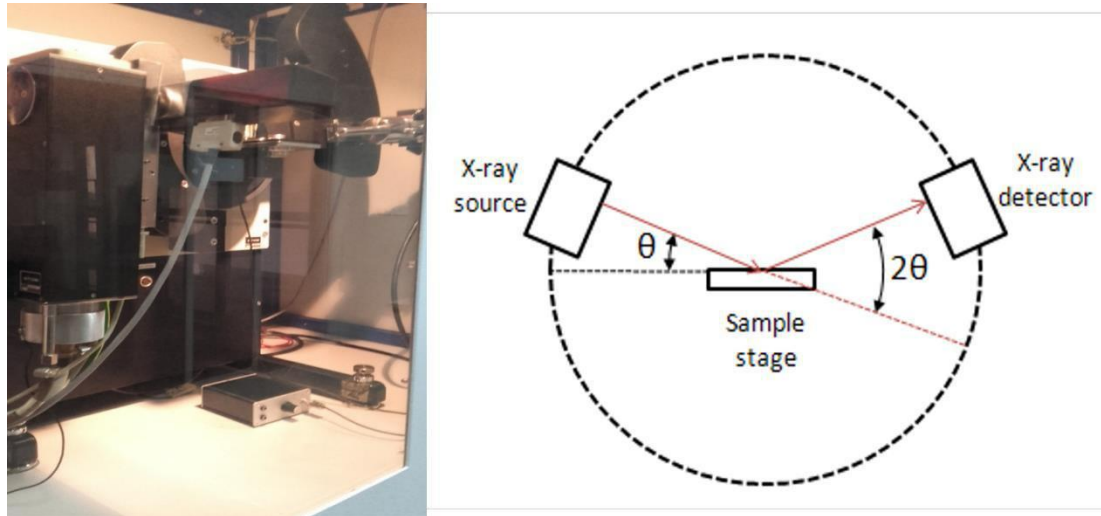


Figure 4-5 a) XRD diffractometer in SCME, NUST b) Schematic of XRD

#### 4.4 Scanning Electron Microscope

In scanning electron microscope, the interaction of electrons with matter is studied to find the topography, composition, particles size and phase mapping of the nano or bulk material. When a high energy electron beam strikes a material, many interactions occur between them which can be used for the analysis of sample.

In scanning electron microscope, the sample surface is scanned by using electron beam and scattered electrons are collected back by the detector which gives information about morphology, particle size and topography. When electron beam interacts with matter surface x-rays, auger electron, back scattered electrons and secondary electrons are generated. Secondary electrons are most commonly used for analysis in SEM. This is because they give very fine image of even small particles of 1 nm. The only requirement for the SEM sample is it should be conductive.

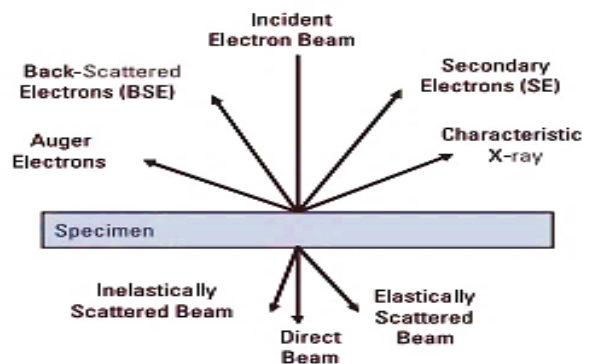


Figure 4-6 Interaction of electronic beam with matter[2]

#### 4.4.1 Instrumentation

- Electron Gun
- Sample chamber
- Detector

The electrons are produced commonly by using thermionic emission method. A set of different type of detectors is used for the collection of emitted electrons and photons when sample interacts with the electron beam. The rastering of electron beam is done by adjusting the X and Y of cathode ray with the X and Y of voltages. As a result of this image is obtained which is saved and used for the topographical and particle size analysis of sample.

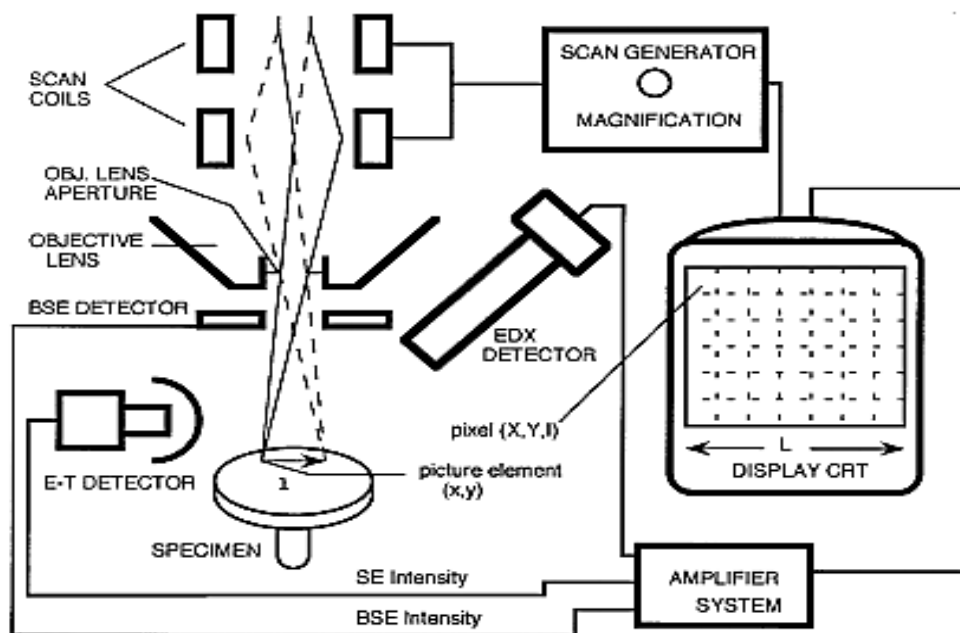


Figure 4-7 Schematic Illustration of working of SEM [3]

#### 4.5 Electrochemical Work Station

Electrochemical workstation provides several techniques (cyclic voltammetry, linear sweep voltammetry, differential pulse voltammetry, square wave voltammetry, chronoamperometry, impedance spectroscopy, etc.) windows-based software, integrated digital CV simulator, impedance simulation and fitting program. These features provide

powerful tools for the understanding of reaction kinetics, trace level analysis, fundamental research, corrosion, energy conversion and storage studies.

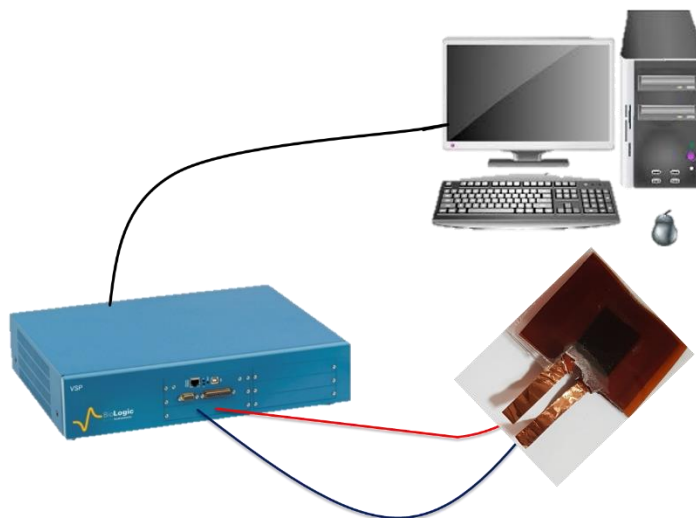


Figure 4-8 Schematic diagram of Electrochemical work station

All the instruments are controlled by EC-Lab® software. It includes all the standard electrochemical techniques such as CV, Amperometry, Potentiometry, Pulsed technique, Electrolysis, ZRA.. EC-Lab® is not only a monitoring software but it includes also analysis tools such as Z Fit (EIS data modeling), CV Fit (voltammetry fitting)



Figure 4-9 Electrochemical impedance spectroscopy setup

# Chapter 5: Results and Discussion

## 5.1 Material Characterization

Material characterization was done by using different techniques to investigate about the properties of material used for device fabrication. Scanning electron microscopy (SEM) was used to know about the morphology of the polyimide and reduced polyimide material. X-ray diffraction (XRD) was used to examine the presence of carbon like material after the reduction of polyimide. Raman spectroscopy and Fourier transform infrared spectroscopy was used for the conformation of reduction of polyimide.

### 5.1.1 Scanning Electron Microscopy

High resolution SEM images of several rPI regions were obtained using a JEOL Analytical SEM (JSM-6490A). Figure 5.1 (a) SEM image in which we can see that when laser passed on the PI substrate it is converted into the reduced PI, the surface morphology of PI gets changed after the irradiation of laser. This image was taken at 35x magnification and Figure 5.1 (b) shows 2500x zoomed image of reduced PI which shows the flakes and porous carbon like material having higher surface density and interconnections with each other. This porous surface look like a honeycomb structure that is useful for storage purposes. The roughened surface with interconnected pores enables excellent electrolyte contact and contributes towards a high capacitance value. Figure 5.1 (c) is taken at 370x magnification which shows the cross-sectional view of reduced PI on PI substrate in this we see that the thickness of reduced PI increased after laser irradiation of PI.

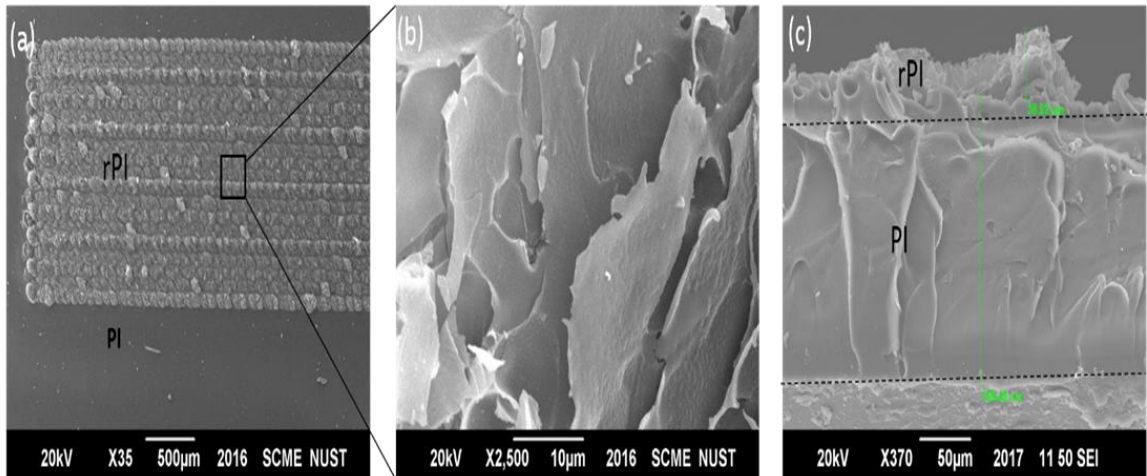


Figure 5-1 SEM images (a) PI and rPI surface; (b) zoomed image of rPI; (c) cross sectional view



### 5.1.2 X-Ray Diffraction Microscopy

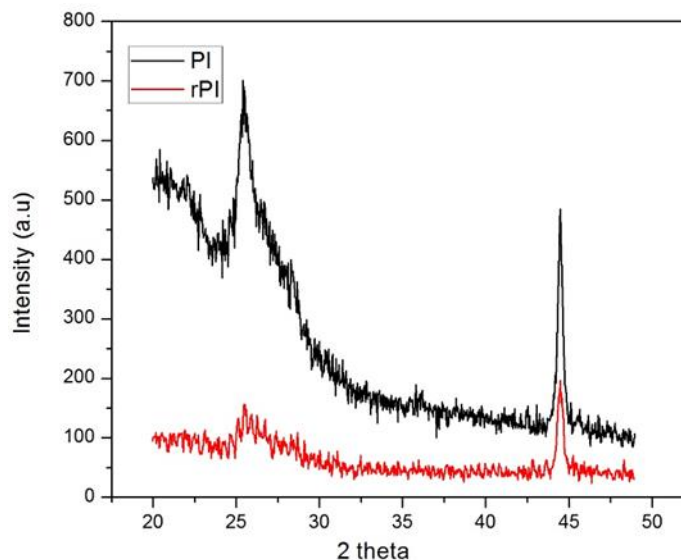


Figure 5-2 XRD image of PI and rPI

X-ray diffraction of PI and reduced PI was done which is shown in Figure 5.2. PI substrate shows a very high intensity peak at  $2\theta$  equal to 25.44. When laser irradiation passed on PI it changes into reduced PI material which shows a very small low intensity peak at  $2\theta$  equal to 25.44. This change in intensity indicates the reduction of PI into the graphene like material. XRD of reduced PI powder was also done. This powder was scraped off from the reduced PI sheet. The peak at  $2\theta$  equal to 24.8 shows that this structure is carbonaceous structure. The peak formed is broader which shows that the structure is graphene like as it is not a very sharp peak.

### 5.1.3 Raman Spectroscopy

The Raman spectrum of polyimide and reduced polyimide is shown in the Figure 5.3. The rPI spectrum shows peaks D at  $1330\text{ cm}^{-1}$ , G at  $1572\text{ cm}^{-1}$  and 2D at  $2700\text{ cm}^{-1}$ . When laser irradiated on polyimide surface due to its heat pyrolysis of PI takes place and it break the bonds between C-O, C=O and C-N and produced carbonaceous and nitric gases. The peaks at point D and G shows the amorphous and graphitic carbon in rPI. G peak at  $1572\text{ cm}^{-1}$  shows the graphitic  $\text{sp}^2$  carbon, D peak at  $1330\text{ cm}^{-1}$  appear due to amorphous carbon or disordered bents present in it and 2D peak at 2700 is appear due to second ordered zone boundary phonon present on rPI surface. Raman spectra was also taken at different points

of rPI. It is seen that the D and G peaks intensities different at different points because the laser temperature dose not remain the same during irradiation and shows irregular behavior. By increasing the laser power, the structure become thicker and porous, but at certain level the intensity of D peak is very high due to which structure get more defects and become disordered.

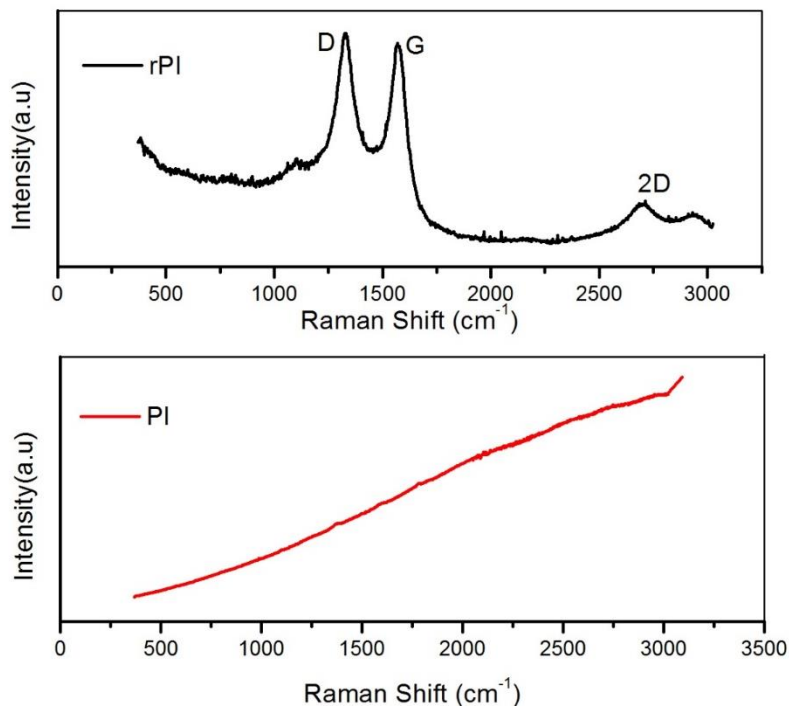


Figure 5-3 Raman Spectroscopy of PI and rPI

#### 5.1.4 Fourier Transform Infrared Spectroscopy

Degradation and reduction process occurs as a result of laser irradiation, which can analyzed via FTIR spectroscopy, which shows the bonds present in a sample. Figure 5.4 shows the FTIR spectra of PI and rPI. It can be seen that for PI the graph comprises of C-O, C-N and C=C stretching and bending peaks in 620-1779  $\text{cm}^{-1}$  region. These peaks disappear in rPI graph as a result of breaking of bonds due to heat provided by irradiating

laser and the aromatic imide present in polyimide act as chromophore group and it absorbs heat to start the de-polymerization reaction.

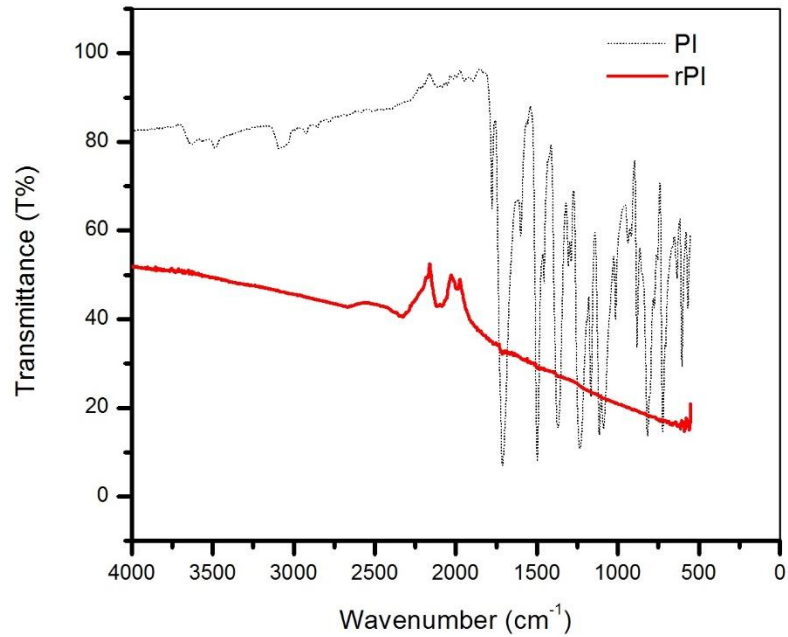


Figure 5-4 FTIR image of PI and rPI

## 5.2 Laser Engraver Characterization

Laser engraver characterization was done in National Center for Physics, Islamabad in the Laser and Optronics Lab. Figure 5.5 shows the image of laser engraver setup and its performance. Figure 5.5 (a) shows the laser device connectivity with computer via USB, Figure 5.5 (b) shows the optical photograph of laser engraver.

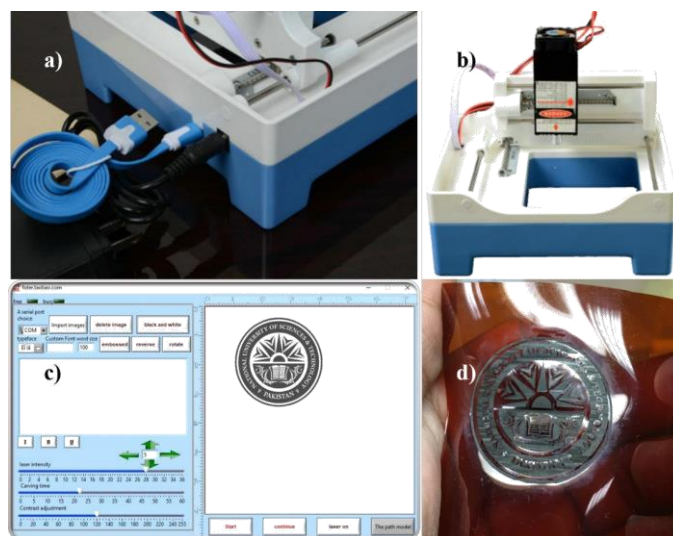


Figure 5-5 a) Laser connections with computer via USB b) The actual laser c) the software laser uses d) Laser scribing over polyimide sheet

Figure 5.5 (c) shows the image of software which is used by laser in this software we import the NUST logo in it. Figure 5.5 (d) shows the image of NUST logo printed on the Polyimide substrate.

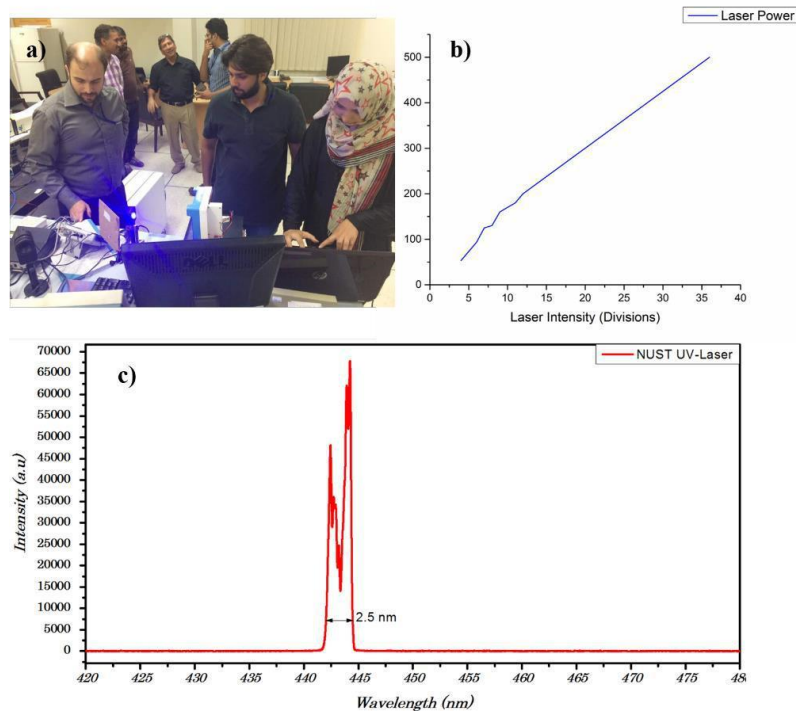


Figure 5-6 a) shows the experiment being conducted at NCP b) Power vs division plot c) Wavelength plot

At NCP different laser device testing was done as shown in Figure 5.6. Laser wavelength and power was tested there. According to the results the wavelength of laser engraver was around 440-445nm while the maximum power of laser was 500mW. In software, laser intensity is shown in 36 levels, across each level laser power was tested.

## 5.3 Device Characterization

### 5.3.1 I-V characterization

Polyimide reduced at different laser intensities I-V characterization was done by using Biologic VSP EC-LAB, in which two probes were used to determine their resistivity. By changing the laser intensity to certain level, the conductivity of the sample increased, after which the conductivity decreased. This shows that there is an optimal power level at which maximum reduction occurs.

Table 8 Reduced PI sample I-V characteristics results.

Sample(Laser Power mW)	Resistivity (k $\Omega$ /m)	Conductivity (mS/m)
138	5.52	0.181
155	4.26	0.234
170	2.41	0.415
185	2.10	0.476
200	4.01	0.249

## 5.4 Supercapacitor Testing

Supercapacitor testing was done by loading sample on EC-Lab set up, in which we attached two probes on supercapacitor terminals. By using its software, we calculated capacitance value. The sample formed and test by doing different changing like:

- 1) By changing Electrolytes
- 2) By changing Laser intensity
- 3) By changing Scan Rates

Electrodes as well as device durability test was also done to know about the efficiency of our device.

### 5.4.1 Conductivity Test

Polyimide is a non-conductive polymer, it behaves like an insulator. When laser passes on the polyimide surface it surfaces changes from brown to black in color. By using digital multi-meter, we check resistance of PI and reduced PI surface. On digital meter we can see that PI show resistance of mega ohms which proves its non-conductive nature, but after laser irradiation reduced polyimide shows a few ohms resistance.

Polyimide and reduced Polyimide conductivity test was also done by using two probe station. Figure 5.7 show the conductivity graph, for finding the conductivity of PI and rPI 0-2V sweep applied. PI shows a maximum current of 0.1pA on output, whereas reduced PI shows a maximum current of 3.2mA on output and a linear graph formed. The relative magnitude of output current and the linear graph shows the conversion of insulating PI

material into the conductive reduced PI material. By using Ohm's law, we find the value of resistance and subsequently calculate the approximate conductance value which is equal to 1.6mS.

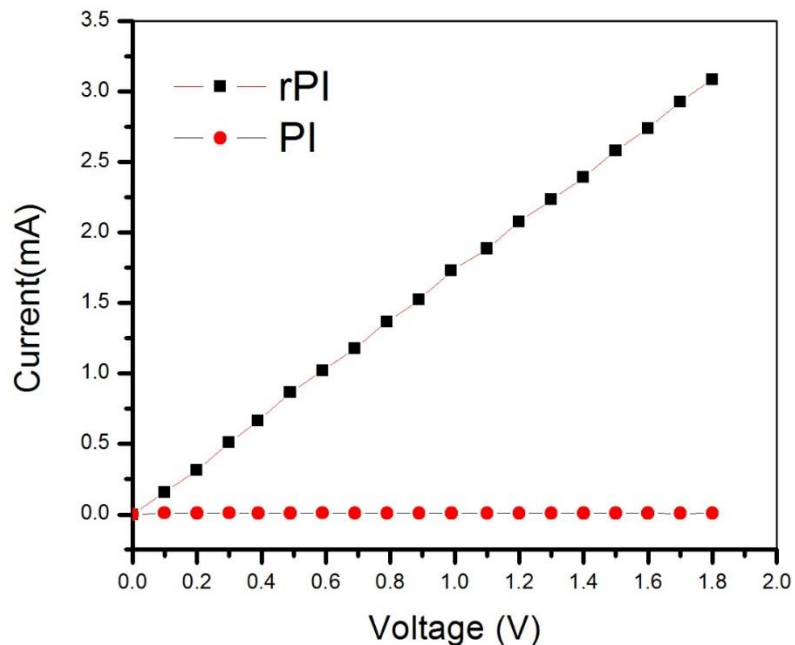


Figure 5-7 Conductivity test of PI and rPI

#### 5.4.2 Electrochemical Testing of Supercapacitor

Supercapacitor capacitance value was done by using different method like by changing the electrolyte, by changing scan rate and by changing laser intensity.

##### 5.4.2.1 Supercapacitor having different Electrolytes

Supercapacitors were fabricated by using different electrolytes like liquid electrolytes and gel electrolytes. By changing electrolyte, the supercapacitor capacitance values get changed. Capacitor capacitance value depends on the electrolyte used in it. The different acidic and basic electrolytes used are potassium hydroxide with water (KOH+H<sub>2</sub>O), phosphoric acid with water (H<sub>3</sub>PO<sub>4</sub>+H<sub>2</sub>O), potassium hydroxide with potassium iodide with polyvinyl alcohol (KOH+KI+PVA) and phosphoric acid with polyvinyl alcohol (H<sub>3</sub>PO<sub>4</sub>+PVA) gel electrolytes.

Figure 5.8 shows the cyclic voltammetry graphs of supercapacitors having different electrolytes. By using EC-lab software we give voltage range from -2V to 2V and a fix scan rate of 20 mV/s to sample electrodes formed at laser intensity of 138mW. From these graphs we can see that the maximum capacitance value we achieved from phosphoric acid with polyvinyl alcohol ( $H_3PO_4$ +PVA) gel electrolyte.

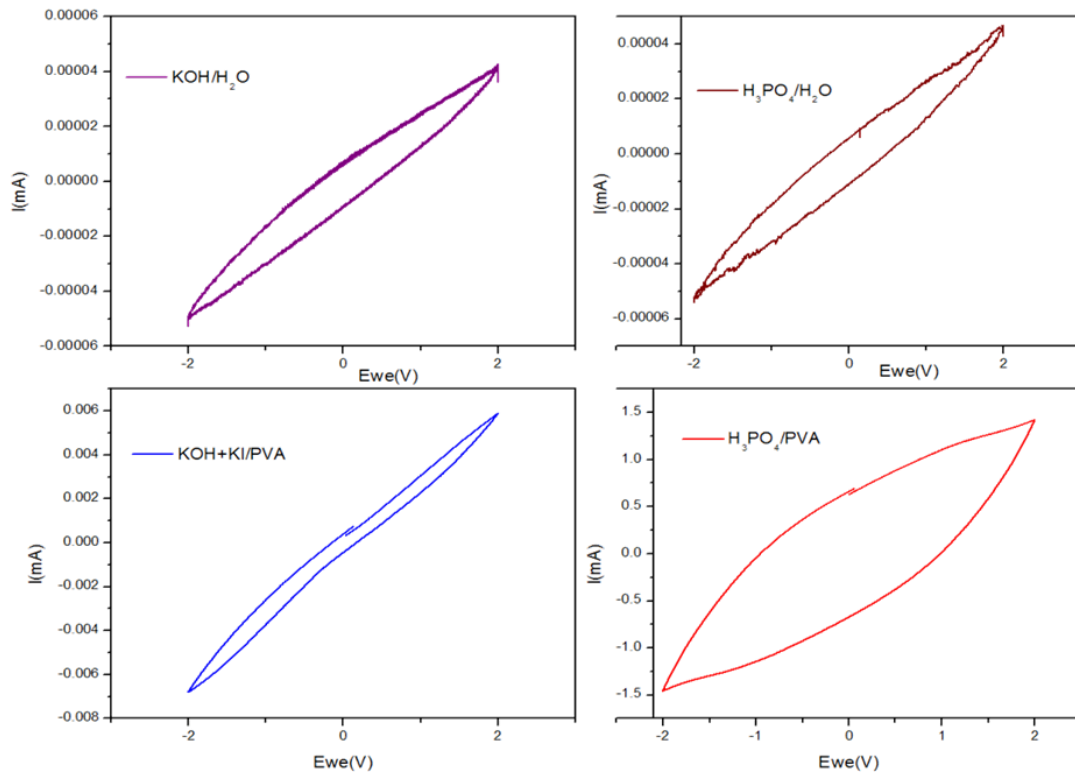


Figure 5-8 Cyclic Voltammetry graphs of different electrolytes at fixed scan rate of 20mV/s

By using different electrolytes the capacitance value get varied due to ions present in the electrolytes. The conductivity of an electrolyte can be define by the number of bare hydrogen ions present in it. The conductivity of  $H^+$ ,  $K^+$  and  $OH^-$  ion is shown in the Figure 3-7 , from this we can see that the  $H^+$  ion have the highest conductivity among the others ion. The  $H_3PO_4$ /PVA shows highest  $75mF/cm^2$  capacitance due to three ions present in it, greater the number of ions the highest the conductivity of electrolyte.

#### 5.4.2.2 Supercapacitor having different Electrolytes and Scan Rates

From Figure 5.9 we can see that by changing the scan rate the capacitance value get changed. We check our device at the scan rate of 20mV/s, 50mV/s and 100mV/s. By changing the scan rate the current value get changed, as we can see that by increasing the scan rate the current value also increased but capacitance value was decreased.

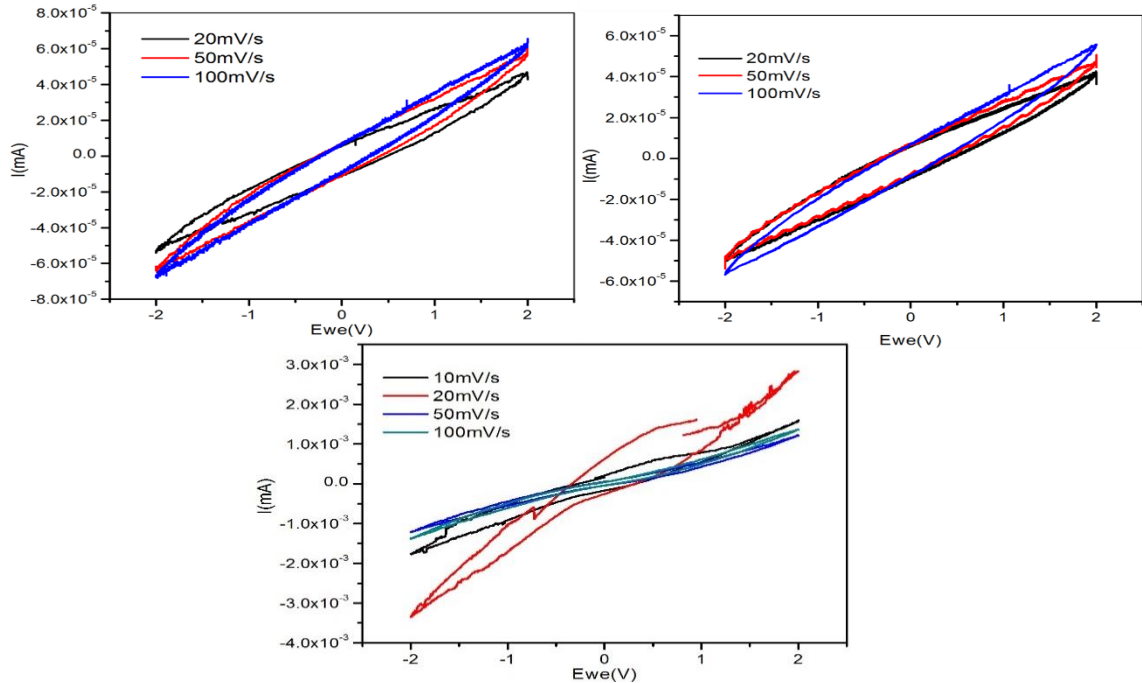


Figure 5-9 Cyclic Voltammetry graphs of different electrolytes at Scan Rate of 20mV/s, 50mV/s and 100mV/s

By increasing the scan rate the diffusion of electrolyte ions into the electrodes internal structure and pore became difficult because voltage sweep that passed onto the electrodes is very fast (diffusion limitation take place) and ineffective interaction between the electrolyte and the electrodes occurs, therefore the at higher scan rate the capacitance value is decrease. So that the specific capacitance and scan rate have inverse relation. At the scan rate of 20mV/s we get the highest capacitance value.



### 5.4.2.3 Supercapacitor having different Laser Intensities and Scan Rates

We fabricate different electrodes by changing the laser intensity of the laser engraver setup that we used. By changing the laser intensity, the resistivity of substrate gets changed. By increasing the laser intensity to a certain value, we see that the resistance value decreases and we get more porous structure. After a certain point in our case above 138mW the resistance of substrate increased because pores got broken, therefore the electrodes formed at higher intensity have discontinuous conductive path.

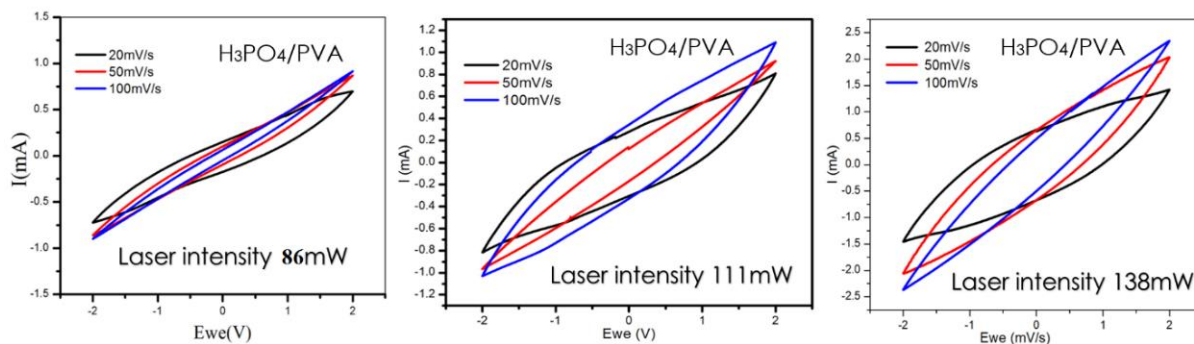


Figure 5-10 Cyclic Voltammetry graphs of different supercapacitor (electrodes formed at different laser intensity) having Phosphoric acid with PVA electrolyte

Figure 5.10 shows the cyclic voltammetry graphs of three different supercapacitor devices having same electrolyte  $H_3PO_4/PVA$  fabricated at different laser intensities of 86mW, 111mW and 138mW respectively were checked at different scan rates. The best result we obtained at laser intensity of 138mW and at scan rate of 20mV/s because this is an optimum laser intensity at which we get highly porous structure. When electrodes have high porosity, electrolyte can diffuse easily on its surface due to which the surface density of the device increased, and high capacitance value can be achieved.

#### 5.4.2.4 Effect of Laser Intensity and Scan rate on Supercapacitor

In Figure 5.11 relation of laser intensity and scan rate with capacitance is shown. Figure 5.11(a, b) both shows the scan rate relation with capacitance, current value increases by increasing the scan rate but the capacitance value decreases at higher scan rate. Figure 5.11(c) show the laser intensity and capacitance relation from which we say that the best capacitance value we achieved at laser intensity of 138mW.

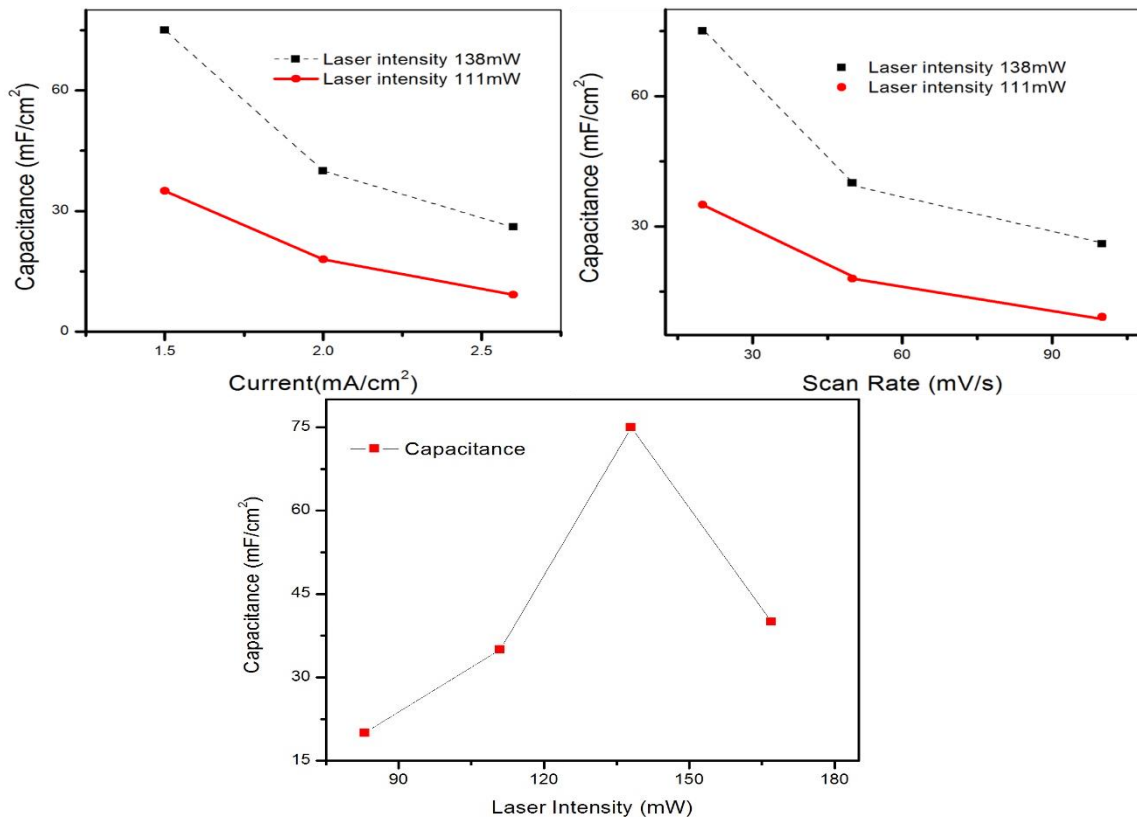


Figure 5-11 Effect of different laser intensity and Scan rate on Capacitance is shown

The physical mechanism of scan rate and laser intensity is described in above sections 5.4.2.2 and 5.4.2.3 respectively. The scan rate relation with the capacitance can also be understood with help of the equation  $C=I/ (dV/dt)$ . Here  $dV/dt$  is the scan rate in mV/s. From this equation and the graph we can see that the scan rate have inverse relation with capacitances. At lower scan rate higher capacitance can be achieved but the current and scan rate have a direct relation, as scan rate increased the current value also increased.

### 5.4.3 Supercapacitor Stability Test

Figure 5.12 (a, c) shows the cyclic voltammetry graphs at different scan rates and laser intensities. Their respective galvanostatic charge and discharge cycles are shown in Figure 5.12(b, d) at different current values which displays symmetric triangular plots throughout with increasing time. These symmetric plots show that the capacitance value of our device have excellent stability. If a device show irregular and non-symmetric graphs that indicate it is not working properly , its charge and discharge timing is different. This non uniform behavior decrease the efficiency of a device. The current density indicated on the graphs shows that at higher current density the faster charge/discharge mechanism take place.

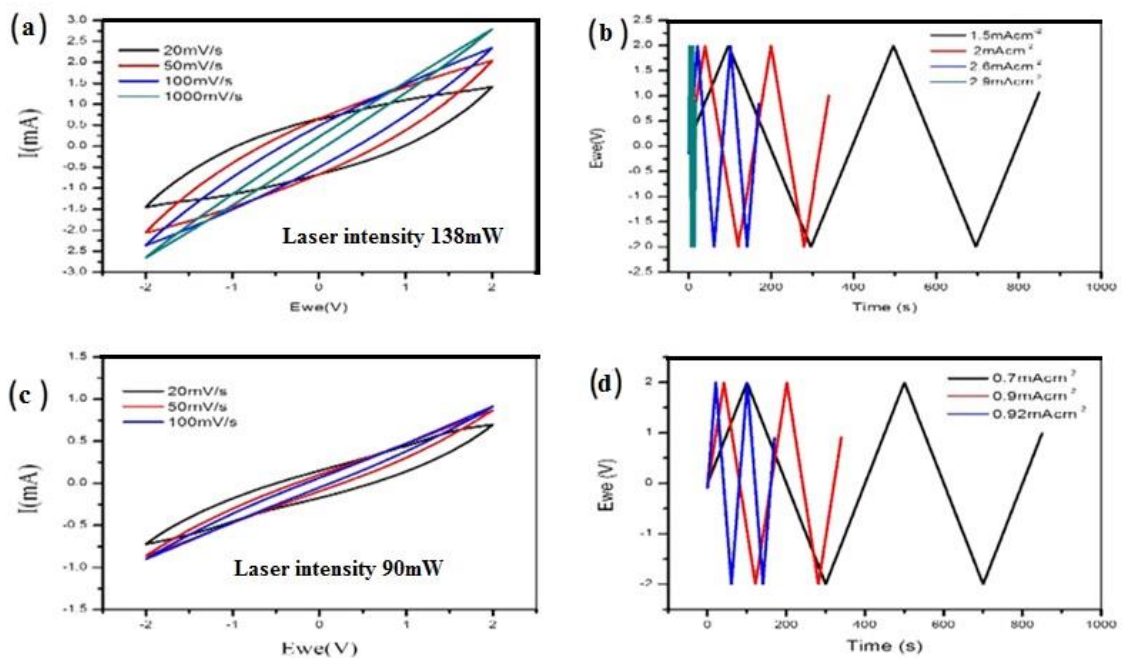


Figure 5-12 Cyclic Voltammetry and galvanostatic charge discharge images (a) CV graphs of supercapacitor electrodes fabricated at laser intensity of 138mW, (b) Charge/discharge graphs of respective supercapacitor shown in (a) ,(c) CV graphs of supercapacitor electrodes fabricated at laser intensity of 90mW ,(d) Charge/discharge graphs of respective supercapacitor shown in (c)

### 5.4.4 Supercapacitor Durability Test

Performance of a device depends on its efficiency and its stability. To check our device performance, we did its retention and efficiency test as shown in the Figure 5.13. Capacitance retention verses no of days graph shown in left image. We check our device constantly around more than 120 days and the capacitance value we achieved was

almost 99.9% same. Efficiency graph is shown in right side image from this we can see that the efficiency value of our device is 99.9% for the no of cycles of more than 360 days.

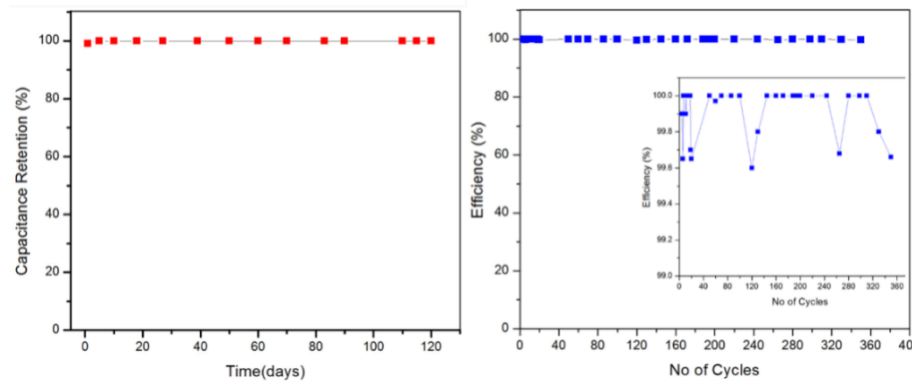


Figure 5-13 Supercapacitor durability and efficiency graphs

Supercapacitor efficiency and durability is define by its constant capacitance value, a device is said to be efficient when after long time it give the same results and its CV graphs remain constant. When a device show change in CV graph that means its storage capacity decreases with time and will not be able to use after some time.

### 5.5 Calculations

For finding the value of capacitance we used the equation (1) and (2)[92], where I is the average current, A is the surface area of the electrodes which is 1cm<sup>2</sup> and dV/dt is the scan rate which is in mV/s.

$$C_{device} = I / (dV/dt) \dots\dots\dots(1)$$

$$C_{areal} = C_{device} / A \dots\dots\dots(2)$$

### Capacitance Value

	Scan Rates	20mV/s	50mV/s	100mV/s
Electrolytes	KOH / H <sub>2</sub> O	2.02μF/cm <sup>2</sup>	0.916μF/cm <sup>2</sup>	0.549μF/cm <sup>2</sup>
	H <sub>3</sub> PO <sub>4</sub> /H <sub>2</sub> O	2.24μF/cm <sup>2</sup>	1.13μF/cm <sup>2</sup>	0.619μF/cm <sup>2</sup>
	KOH+KI/PVA	0.23mF/cm <sup>2</sup>	25μF/cm <sup>2</sup>	12μF/cm <sup>2</sup>
	H <sub>3</sub> PO <sub>4</sub> /PVA	75mF/cm <sup>2</sup>	34mF/cm <sup>2</sup>	21mF/cm <sup>2</sup>

Figure 5-14 Supercapacitor having different electrolyte capacitance values at different scan rates.

The capacitance value we calculated here is the areal capacitance. We calculated the value of capacitance also by using equation (3), in which we calculated capacitance from the

CV curve. Here I(V) is the total current enclosed in CV curve which is in mA, S is the specific active area of the electrodes which is 1cm<sup>2</sup> in it dV/dt is the scan rate which is in mV/s and V<sub>f</sub> and V<sub>i</sub> are the voltage limits.

$$C_A = \frac{1}{2 \times S \times (v_f - v_i) \times \frac{dV}{dt}} \int_{v_i}^{v_f} I(V) dV \dots\dots\dots (3)$$

We calculated the specific areal capacitance (C<sub>A</sub> in mF/cm<sup>2</sup>). We can also calculate the volumetric capacitance (C<sub>v</sub> in mF/cm<sup>3</sup>) by using equation (4).

$$C_v = C_A / d \dots\dots\dots (4)$$

C<sub>A</sub> is the specific areal capacitance that we calculated by using above equations, d is the thickness of the active electrodes material.

The specific areal (E<sub>A</sub> in μWhcm<sup>-2</sup>) and volumetric energy density (E<sub>v</sub> in μWhm<sup>-3</sup>) can be calculated using equations (5) and (6).

$$E_A = \frac{1}{2} \times C_A \times (V_{max} - V_{drop})^2 / 3600 \dots\dots\dots (5)$$

$$E_v = \frac{1}{2} \times C_v \times (V_{max} - V_{drop})^2 / 3600 \dots\dots\dots (6)$$

V<sub>max</sub> is the maximum voltage applied and V<sub>drop</sub> is the voltage drop indicated from the first two data points in the discharge curves. Table 9 shows the literature capacitance values, from this it is clear that capacitance not depend on one factor, there are many things due to which capacitance value get changed.

Table 9 Literature comparison of capacitance value

Capacitance	Electrolyte	Electrode Material	Paper
16.5mF/cm <sup>2</sup>	PVA/H <sub>2</sub> SO <sub>4</sub>	Boron doped induced graphene interdigitated	<b>DOI:</b> 10.1021/acsnano.5b00436
>9mF/cm <sup>2</sup>	PVA/H <sub>2</sub> SO <sub>4</sub>	Polyimide stacked	<b>DOI:</b> 10.1021/am509065d
4mF/cm <sup>2</sup>	Aqueous H <sub>2</sub> SO <sub>4</sub>	Laser induced interdigitated electrodes	<b>DOI:</b> 10.1038/ncomms6714
2.6-3.7mF/cm <sup>2</sup>	0.09mol H <sub>3</sub> PO <sub>4</sub> -PVA	Graphene based	<b>DOI:</b> 10.1039/C4RA05553E
1.5mF/cm <sup>2</sup> for GO reduction 4mF/cm <sup>2</sup> for PI reduction	PVA/H <sub>2</sub> SO <sub>4</sub>	GO, PI electrodes laser reduction by DVD burner	<b>DOI:</b> 10.13140/RG.2.1.1425.624 3
0.8mF/cm <sup>2</sup>	PVA/H <sub>3</sub> PO <sub>4</sub>	Polyimide Interdigitated electrodes	<b>DOI:</b> 10.1016/j.carbon.2014.11.017

## Conclusions

In this work, we have reported the fabrication and characterization of a supercapacitor which uses laser reduced polyimide as the electrodes. Laser reduction is a low cost and relatively straightforward method to reduce PI and convert a surface layer into a carbonized material having high porosity. Reduced PI has a high storage capacity and we have analyzed the performance of our device by using different electrolytes (KOH/H<sub>2</sub>O, H<sub>3</sub>PO<sub>4</sub>/H<sub>2</sub>O, KOH+KI/PVA, H<sub>3</sub>PO<sub>4</sub>/PVA). Supercapacitor electrodes were formed by varying the laser intensity from 83mW to 167mW. We found that 138mW is the optimum power for the stacked supercapacitor geometry on a 200μm thick PI substrate. The maximum capacitance value of 75mF/cm<sup>2</sup> was obtained by using H<sub>3</sub>PO<sub>4</sub>/PVA electrolyte between the electrodes formed at 138mW. From this we concluded that by changing the electrolytes and intensity of the laser to an optimum condition one can change the capacitance value. Further, by increasing the laser intensity, the capacitance value increased. At different scan rates supercapacitor was tested, at lower scan rate the current value was lower but capacitance value was higher. By varying the scan rate we concluded that scan rate and capacitance value have inverse relationship. At lower scan rate we achieved higher capacitance value and at higher scan rate capacitance value decreased. The stability test of supercapacitor was done which shows 99% stability of device for more than 350 cycles.

## Recommendations

- In future supercapacitor of different sizes, shapes and geometry can be fabricated using the same laser scribing technology.
- By using this single step technique, we can also fabricate interdigitated supercapacitor.
- We can also study the effect of electric field on capacitance by varying the electrode size and distance between the interdigitated electrodes.
- The effect of conductive electrolyte ions on capacitances can also be studied.
- Ionic liquid as an electrolyte for supercapacitor is also recommended for future experiments.
- Comparison between organic and inorganic electrolytes can also be done, by this one can know about the better capacitance value and stability of supercapacitor.
- We can also calculate the energy and power density of our devices.



## References

- [1] D. Harvey, *Modern analytical chemistry* vol. 381: McGraw-Hill New York, 2000.
- [2] Z. Guo and L. Tan, *Fundamentals and applications of nanomaterials*: Artech House, 2009.
- [3] J. D. Thompson, *Organizations in action: Social science bases of administrative theory*: Routledge, 2017.
- [4] M. D. Stewart, K. Patterson, M. H. Somervell, and C. G. Willson, "Organic imaging materials: a view of the future," *Journal of Physical Organic Chemistry*, vol. 13, pp. 767-774, 2000.
- [5] J. Hu, "Overview of flexible electronics from ITRI's viewpoint," in *VLSI Test Symposium (VTS), 2010 28th*, 2010, pp. 84-84.
- [6] I.-C. Cheng and S. Wagner, "Overview of flexible electronics technology," in *Flexible Electronics*, ed: Springer, 2009, pp. 1-28.
- [7] D. B. Mitzi, L. L. Kosbar, C. E. Murray, M. Copel, and A. Afzali, "High-mobility ultrathin semiconducting films prepared by spin coating," *Nature*, vol. 428, p. 299, 2004.
- [8] P. T. Kazlas and M. D. McCreary, "Paperlike microencapsulated electrophoretic materials and displays," *MRS bulletin*, vol. 27, pp. 894-897, 2002.
- [9] M.-C. Choi, J. Wakita, C.-S. Ha, and S. Ando, "Highly transparent and refractive polyimides with controlled molecular structure by chlorine side groups," *Macromolecules*, vol. 42, pp. 5112-5120, 2009.
- [10] A. Plichta, A. Habeck, S. Knoche, A. Kruse, A. Weber, and N. Hildebrand, "Flexible glass substrates," *Flexible Flat Panel Displays*, vol. 3, p. 35, 2005.
- [11] Y. Chen, J. Au, P. Kazlas, A. Ritenour, H. Gates, and M. McCreary, "Electronic paper: Flexible active-matrix electronic ink display," *Nature*, vol. 423, p. 136, 2003.
- [12] W. A. MacDonald, "Engineered films for display technologies," *Journal of Materials Chemistry*, vol. 14, pp. 4-10, 2004.
- [13] M. Goosey, "Permeability of coatings and encapsulants for electronic and optoelectronic devices," in *Polymer Permeability*, ed: Springer, 1985, pp. 309-339.

- [14] E. Jamieson and A. Windle, "Structure and oxygen-barrier properties of metallized polymer film," *Journal of Materials Science*, vol. 18, pp. 64-80, 1983.
- [15] B. D. Vogt, H.-J. Lee, V. M. Prabhu, D. M. DeLongchamp, E. K. Lin, W.-I. Wu, *et al.*, "X-ray and neutron reflectivity measurements of moisture transport through model multilayered barrier films for flexible displays," *Journal of applied physics*, vol. 97, p. 114509, 2005.
- [16] P. E. Burrows, G. L. Graff, M. E. Gross, P. M. Martin, M.-K. Shi, M. Hall, *et al.*, "Ultra barrier flexible substrates for flat panel displays," *Displays*, vol. 22, pp. 65-69, 2001.
- [17] N. G. McCrum, C. Buckley, C. B. Bucknall, and C. Bucknall, *Principles of polymer engineering*: Oxford University Press, USA, 1997.
- [18] K. Long, A. Kattamis, I.-C. Cheng, H. Gleskova, S. Wagner, J. Sturm, *et al.*, "Active-Matrix Amorphous-Silicon TFTs Arrays at 180°C on Clear Plastic and Glass Substrates for Organic Light-Emitting Displays," *IEEE Transactions on Electron Devices*, vol. 53, pp. 1789-1796, 2006.
- [19] H. Chatham, "Oxygen diffusion barrier properties of transparent oxide coatings on polymeric substrates," *Surface and Coatings Technology*, vol. 78, pp. 1-9, 1996.
- [20] W. Liu, D. Lin, A. Pei, and Y. Cui, "Stabilizing lithium metal anodes by uniform Li-ion flux distribution in nanochannel confinement," *Journal of the American Chemical Society*, vol. 138, pp. 15443-15450, 2016.
- [21] C. Sroog, "Polyimides," *Progress in Polymer Science*, vol. 16, pp. 561-694, 1991.
- [22] G. Bower and L. Frost, "Aromatic polyimides," *Journal of Polymer Science Part A: General Papers*, vol. 1, pp. 3135-3150, 1963.
- [23] L. Frost and I. Kesse, "Spontaneous degradation of aromatic polypromellitic acids," *Journal of Applied Polymer Science*, vol. 8, pp. 1039-1051, 1964.
- [24] C. Sroog, A. Endrey, S. Abramo, C. Berr, W. Edwards, and K. Olivier, "Aromatic polypyromellitimides from aromatic polyamic acids," *Journal of Polymer Science Part A: Polymer Chemistry*, vol. 34, pp. 2069-2086, 1996.
- [25] S. Vinogradova, Y. S. Vygodskii, V. Vorob'ev, N. Churochkina, L. Chudina, T. Spirina, *et al.*, "Chemical cyclization of poly (amido-acids) in solution," *Polymer Science USSR*, vol. 16, pp. 584-589, 1974.

- [26] R. Dine-Hart and W. Wright, "Preparation and fabrication of aromatic polyimides," *Journal of Applied Polymer Science*, vol. 11, pp. 609-627, 1967.
- [27] C. Sroog, "Polyimides," *Journal of Polymer Science: Macromolecular Reviews*, vol. 11, pp. 161-208, 1976.
- [28] B. D. Gates, Q. Xu, M. Stewart, D. Ryan, C. G. Willson, and G. M. Whitesides, "New approaches to nanofabrication: molding, printing, and other techniques," *Chemical reviews*, vol. 105, pp. 1171-1196, 2005.
- [29] B. J. Kim and E. Meng, "Review of polymer MEMS micromachining," *Journal of Micromechanics and Microengineering*, vol. 26, p. 013001, 2015.
- [30] J. van Schoot, K. Troost, F. Bornebroek, R. van Ballegoij, S. Lok, P. Krabbendam, *et al.*, "High-NA EUV lithography enabling Moore's law in the next decade," in *International Conference on Extreme Ultraviolet Lithography 2017*, 2017, p. 104500U.
- [31] P. van Assenbergh, E. Meinders, J. Geraedts, and D. Dodou, "Nanostructure and Microstructure Fabrication: From Desired Properties to Suitable Processes," *Small*, vol. 14, p. 1703401, 2018.
- [32] T. Shimoda, Y. Matsuki, M. Furusawa, T. Aoki, I. Yudasaka, H. Tanaka, *et al.*, "Solution-processed silicon films and transistors," *Nature*, vol. 440, p. 783, 2006.
- [33] F. Garnier, R. Hajlaoui, A. Yassar, and P. Srivastava, "All-polymer field-effect transistor realized by printing techniques," *Science*, vol. 265, pp. 1684-1686, 1994.
- [34] H. Gau, S. Herminghaus, P. Lenz, and R. Lipowsky, "Liquid morphologies on structured surfaces: from microchannels to microchips," *Science*, vol. 283, pp. 46-49, 1999.
- [35] B. A. Ridley, B. Nivi, and J. M. Jacobson, "All-inorganic field effect transistors fabricated by printing," *Science*, vol. 286, pp. 746-749, 1999.
- [36] T. N. Ng, R. A. Lujan, S. Sambandan, R. A. Street, S. Limb, and W. S. Wong, "Low temperature a-Si: H photodiodes and flexible image sensor arrays patterned by digital lithography," *Applied Physics Letters*, vol. 91, p. 063505, 2007.
- [37] H. Gleskova, S. Wagner, and D. Shen, "Electrophotographic patterning of thin-film silicon on glass foil," *IEEE Electron Device Letters*, vol. 16, pp. 418-420, 1995.

- [38] C. Liu, F. Li, L. P. Ma, and H. M. Cheng, "Advanced materials for energy storage," *Advanced materials*, vol. 22, pp. E28-E62, 2010.
- [39] A. Pandolfo and A. Hollenkamp, "Carbon properties and their role in supercapacitors," *Journal of power sources*, vol. 157, pp. 11-27, 2006.
- [40] J. R. Miller and P. Simon, "Electrochemical capacitors for energy management," *Science Magazine*, vol. 321, pp. 651-652, 2008.
- [41] A. S. Arico, P. Bruce, B. Scrosati, J.-M. Tarascon, and W. Van Schalkwijk, "Nanostructured materials for advanced energy conversion and storage devices," in *Materials For Sustainable Energy: A Collection of Peer-Reviewed Research and Review Articles from Nature Publishing Group*, ed: World Scientific, 2011, pp. 148-159.
- [42] S. Roundy, P. K. Wright, and J. Rabaey, "A study of low level vibrations as a power source for wireless sensor nodes," *Computer communications*, vol. 26, pp. 1131-1144, 2003.
- [43] W. Chen, M. Beidaghi, V. Penmatsa, K. Bechtold, L. Kumari, W. Li, *et al.*, "Integration of carbon nanotubes to C-MEMS for on-chip supercapacitors," *IEEE Transactions on Nanotechnology*, vol. 9, pp. 734-740, 2010.
- [44] J. Mayer, P. V. Borges, and S. J. Simske, "Introduction," in *Fundamentals and Applications of Hardcopy Communication*, ed: Springer, 2018, pp. 1-5.
- [45] M. L. Trudeau, "Advanced materials for energy storage," *Mrs Bulletin*, vol. 24, pp. 23-26, 1999.
- [46] M. Jayalakshmi and K. Balasubramanian, "Simple capacitors to supercapacitors-an overview," *Int. J. Electrochem. Sci*, vol. 3, pp. 1196-1217, 2008.
- [47] M. V. Kiamahalleh, S. H. S. Zein, G. Najafpour, S. A. Sata, and S. Buniran, "Multiwalled carbon nanotubes based nanocomposites for supercapacitors: a review of electrode materials," *Nano*, vol. 7, p. 1230002, 2012.
- [48] M. S. Halper and J. C. Ellenbogen, "Supercapacitors: A brief overview," *MITRE Nanosystems Group*, 2006.
- [49] H. Choi and H. Yoon, "Nanostructured electrode materials for electrochemical capacitor applications," *Nanomaterials*, vol. 5, pp. 906-936, 2015.

- [50] P. Simon and Y. Gogotsi, "Materials for electrochemical capacitors," in *Nanoscience And Technology: A Collection of Reviews from Nature Journals*, ed: World Scientific, 2010, pp. 320-329.
- [51] S. Mohapatra, A. Acharya, and G. Roy, "The role of nanomaterial for the design of supercapacitor," *Lat Am J Phys Educ*, vol. 6, pp. 380-384, 2012.
- [52] Q. Chen, X. Li, X. Zang, Y. Cao, Y. He, P. Li, *et al.*, "Effect of different gel electrolytes on graphene-based solid-state supercapacitors," *RSC Advances*, vol. 4, pp. 36253-36256, 2014.
- [53] A. Burke, "R&D considerations for the performance and application of electrochemical capacitors," *Electrochimica Acta*, vol. 53, pp. 1083-1091, 2007.
- [54] A. Burke, Z. Liu, and H. Zhao, "Present and future applications of supercapacitors in electric and hybrid vehicles," in *Electric Vehicle Conference (IEVC), 2014 IEEE International*, 2014, pp. 1-8.
- [55] Z. Bo, Z. Wen, H. Kim, G. Lu, K. Yu, and J. Chen, "One-step fabrication and capacitive behavior of electrochemical double layer capacitor electrodes using vertically-oriented graphene directly grown on metal," *Carbon*, vol. 50, pp. 4379-4387, 2012.
- [56] A. P. Singh, N. K. Tiwari, P. Karandikar, and A. Dubey, "Effect of electrode shape on the parameters of supercapacitor," in *Industrial Instrumentation and Control (ICIC), 2015 International Conference on*, 2015, pp. 669-673.
- [57] H. Yang, S. Kannappan, A. S. Pandian, J.-H. Jang, Y. S. Lee, and W. Lu, "Nanoporous graphene materials by low-temperature vacuum-assisted thermal process for electrochemical energy storage," *Journal of Power Sources*, vol. 284, pp. 146-153, 2015.
- [58] N. Syarif, T. Ivandini, and W. Wibowoa, "Direct synthesis carbon/metal oxide composites for electrochemical capacitors electrode," *Trans J Eng Manag Appl Sci Technol*, vol. 3, p. 2, 2011.
- [59] Q. Cheng, J. Tang, J. Ma, H. Zhang, N. Shinya, and L.-C. Qin, "Graphene and carbon nanotube composite electrodes for supercapacitors with ultra-high energy density," *Physical Chemistry Chemical Physics*, vol. 13, pp. 17615-17624, 2011.

- [60] C. Du and N. Pan, "C. Du and N. Pan, Carbon nanotube-based supercapacitors, *Nanotech. Law Business* 4, 569 (2007)," *Nanotech. Law Business*, vol. 4, p. 569, 2007.
- [61] P. Tamilarasan, A. K. Mishra, and S. Ramaprabhu, "Graphene/ionic liquid binary electrode material for high performance supercapacitor," in *Nanoscience, Technology and Societal Implications (NSTSI), 2011 International Conference on*, 2011, pp. 1-5.
- [62] E. G. Bakhoun and M. H. Cheng, "Capacitive pressure sensor with very large dynamic range," *IEEE Transactions on Components and Packaging Technologies*, vol. 33, pp. 79-83, 2010.
- [63] C. Liu, Z. Yu, D. Neff, A. Zhamu, and B. Z. Jang, "Graphene-based supercapacitor with an ultrahigh energy density," *Nano letters*, vol. 10, pp. 4863-4868, 2010.
- [64] P. Karthika, N. Rajalakshmi, and K. S. Dhathathreyan, "Functionalized exfoliated graphene oxide as supercapacitor electrodes," *Soft Nanoscience Letters*, vol. 2, p. 59, 2012.
- [65] T. Kim, G. Jung, S. Yoo, K. S. Suh, and R. S. Ruoff, "Activated graphene-based carbons as supercapacitor electrodes with macro-and mesopores," *ACS nano*, vol. 7, pp. 6899-6905, 2013.
- [66] S. Hornblower, A. Spawforth, and E. Eidinow, *The Oxford classical dictionary*: Oxford University Press, 2012.
- [67] Z. S. Iro, C. Subramani, and S. Dash, "A brief review on electrode materials for supercapacitor," *Int. J. Electrochem. Sci*, vol. 11, pp. 10628-10643, 2016.
- [68] A. Namisnyk, "University of Technology," ed: Sydney, 2003.
- [69] D.-W. Wang, F. Li, J. Zhao, W. Ren, Z.-G. Chen, J. Tan, *et al.*, "Fabrication of graphene/polyaniline composite paper via in situ anodic electropolymerization for high-performance flexible electrode," *ACS nano*, vol. 3, pp. 1745-1752, 2009.
- [70] E. Frackowiak, V. Khomenko, K. Jurewicz, K. Lota, and F. Béguin, "Supercapacitors based on conducting polymers/nanotubes composites," *Journal of Power Sources*, vol. 153, pp. 413-418, 2006.

- [71] K. Jurewicz, S. Delpoux, V. Bertagna, F. Beguin, and E. Frackowiak, "Supercapacitors from nanotubes/polypyrrole composites," *Chemical Physics Letters*, vol. 347, pp. 36-40, 2001.
- [72] N. Kaempfen, "Stowable mezzanine bed," ed: Google Patents, 2009.
- [73] X.-L. Qi and S.-C. Zhang, "Topological insulators and superconductors," *Reviews of Modern Physics*, vol. 83, p. 1057, 2011.
- [74] S. P. Singh, S. Ramanan, Y. Kaufman, and C. J. Arnusch<sup>1</sup>, "Laser-Induced Graphene Biofilm Inhibition: Texture Does Matter," *ACS Applied Nano Materials*, vol. 1, pp. 1713-1720, 2018.
- [75] Y. Zhang, L. Guo, S. Wei, Y. He, H. Xia, Q. Chen, *et al.*, "Direct imprinting of microcircuits on graphene oxides film by femtosecond laser reduction," *Nano Today*, vol. 5, pp. 15-20, 2010.
- [76] H. Tian, Y. Yang, D. Xie, Y.-L. Cui, W.-T. Mi, Y. Zhang, *et al.*, "Wafer-scale integration of graphene-based electronic, optoelectronic and electroacoustic devices," *Scientific reports*, vol. 4, p. 3598, 2014.
- [77] N.-Q. Deng, H. Tian, Z.-Y. Ju, H.-M. Zhao, C. Li, M. A. Mohammad, *et al.*, "Tunable graphene oxide reduction and graphene patterning at room temperature on arbitrary substrates," *Carbon*, vol. 109, pp. 173-181, 2016.
- [78] J. Lin, Z. Peng, Y. Liu, F. Ruiz-Zepeda, R. Ye, E. L. Samuel, *et al.*, "Laser-induced porous graphene films from commercial polymers," *Nature communications*, vol. 5, p. 5714, 2014.
- [79] B. Dorin, P. Parkinson, and P. Scully, "Direct laser write process for 3D conductive carbon circuits in polyimide," *Journal of Materials Chemistry C*, vol. 5, pp. 4923-4930, 2017.
- [80] A. Lamberti, M. Serrapede, G. Ferraro, M. Fontana, F. Perrucci, S. Bianco, *et al.*, "All-SPEEK flexible supercapacitor exploiting laser-induced graphenization," *2D Materials*, vol. 4, p. 035012, 2017.
- [81] M. Inagaki, N. Ohta, and Y. Hishiyama, "Aromatic polyimides as carbon precursors," *Carbon*, vol. 61, pp. 1-21, 2013.
- [82] A. Mühlebach, B. Müller, C. Pharisa, M. Hofmann, B. Seiferling, and D. Guerry, "New water-soluble photo crosslinkable polymers based on modified poly (vinyl

- alcohol)," *Journal of Polymer Science Part A: Polymer Chemistry*, vol. 35, pp. 3603-3611, 1997.
- [83] M. Hema, S. Selvasekarapandian, H. Nithya, A. Sakunthala, and D. Arunkumar, "Structural and ionic conductivity studies on proton conducting polymer electrolyte based on polyvinyl alcohol," *Ionics*, vol. 15, pp. 487-491, 2009.
- [84] S. Moulay, "Poly (vinyl alcohol) Functionalizations and Applications," *Polymer-Plastics Technology and Engineering*, vol. 54, pp. 1289-1319, 2015.
- [85] M. Krumova, D. Lopez, R. Benavente, C. Mijangos, and J. Perena, "Effect of crosslinking on the mechanical and thermal properties of poly (vinyl alcohol)," *Polymer*, vol. 41, pp. 9265-9272, 2000.
- [86] L.-Q. Tao, H. Tian, Y. Liu, Z.-Y. Ju, Y. Pang, Y.-Q. Chen, *et al.*, "An intelligent artificial throat with sound-sensing ability based on laser induced graphene," *Nature Communications*, vol. 8, p. 14579, 2017.
- [87] M. Rosi, F. Iskandar, M. Abdullah, and Khairurrijal, "Hydrogel-polymer electrolytes based on polyvinyl alcohol and hydroxyethylcellulose for supercapacitor applications," *International Journal of Electrochemical Science*, vol. 9, pp. 4251-4256, 2014.
- [88] M. Kaempgen, C. K. Chan, J. Ma, Y. Cui, and G. Gruner, "Printable thin film supercapacitors using single-walled carbon nanotubes," *Nano letters*, vol. 9, pp. 1872-1876, 2009.
- [89] C.-C. Yang, S.-T. Hsu, and W.-C. Chien, "All solid-state electric double-layer capacitors based on alkaline polyvinyl alcohol polymer electrolytes," *Journal of power sources*, vol. 152, pp. 303-310, 2005.
- [90] H. Yu, J. Wu, L. Fan, K. Xu, X. Zhong, Y. Lin, *et al.*, "Improvement of the performance for quasi-solid-state supercapacitor by using PVA–KOH–KI polymer gel electrolyte," *Electrochimica Acta*, vol. 56, pp. 6881-6886, 2011.
- [91] D. A. Skoog, F. J. Holler, and S. R. Crouch, *Principles of instrumental analysis*: Cengage learning, 2017.
- [92] J. Lin, C. Zhang, Z. Yan, Y. Zhu, Z. Peng, R. H. Hauge, *et al.*, "3-dimensional graphene carbon nanotube carpet-based microsupercapacitors with high electrochemical performance," *Nano letters*, vol. 13, pp. 72-78, 2012.



